THE EFFECTS OF CHAMBER GEOMETRY, SURFACE CHARACTERISTICS, AND TEMPERATURE BOUNDARY CONDITIONS ON THE HYDROGEN-OXYGEN REACTION

Thesis by

Craig Marks

In Partial Fulfillment of the Requirements

for the Degree of

Doctor of Philosophy

California Institute of Technology

Pasadena, California

1955

ACKNOWLEDGEMENTS

The author wishes to express his sincere appreciation to Dr. Peter Kyropoulos for his encouragement, council and aid, without which this investigation would have been impossible. Dr. Oliver Wulf and Dr. Norman Davidson have been more than generous in devoting their time to many discussions concerning this work. Thanks are also due Dr. David Wood for his many suggestions during the preliminary design stages.

ABSTRACT

The established mechanism of the hydrogen-oxygen reaction is reviewed and calculated results presented concerning the rates of reaction and the explosion temperatures expected with various concentrations of water vapor. A simplified theory is developed to predict the overall rate of reaction in the case where a strong temperature gradient exists. Experiments are described in which stoichiometric mixtures of hydrogen and oxygen are introduced to a closed, shallow, nickel plated, cylindrical combustion chamber and measurements made of the pressure change with time. The top surface of the chamber is heated while the bottom surface is either heated or cooled to provide isothermal or gradient conditions, respectively. A large catalytic reaction due to the nickel surfaces is observed. The measured reaction rates and the conditions for explosion with isothermal heating are consistent with predictions based on the established reaction scheme. With gradient heating the rates measured are larger than those predicted by the simplified theory with temperatures of the top surface above 1300°R. This fact is believed to be caused by the diffusion of active intermediate reaction products from hot regions into the cooler reactants. These intermediate products are neglected in the simplified analysis. No explosion was observed with gradient heating even when the hot plate was above the temperature which caused isothermal explosion. This fact is explained on the basis of the strong inhibiting effect which water vapor exhibits toward the hydrogen-oxygen reaction.

TABLE OF CONTENTS

Part	Title	Page
	ACKNOWLEDGEMENTS	i
	ABSTRACT	ii
	LIST OF FIGURES	iv
I	INTRODUCTION	1
II	PREDICTION OF REACTION RATES	7
III	EQUIPMENT	30
IV	TEST PROCEDURE	46
V	EXPERIMENTAL RESULTS	51
VI	DISCUSSION	59
VII	CONCLUSIONS	66
	APPENDIX	67
	REFERENCES	68

LIST OF FIGURES

Figure No.	Title	Page
1	Explosion Limits for Hydrogen-Oxygen Mixture	2
2	Explosion Limit Curves for Various Surfaces	12
3	Effect of Vessel Size and Water Vapor Concentration on Explosion Temperature	17
4	Effect of Water Vapor on the Reaction Rate	18
5	General View of Combustion Chamber	34
6	One-Quarter Cross-section Drawing of Chamber	35
7	Outside View of Chamber	36
8	Upper Heating Plate	36
9	Heater Controls and Temperature Recorder	37
10	Pressure Transducers	37
11	Top Side of Lower Heating Pot	40
12	Bottom Side of Lower Heating Pot	40
13	Top Side of Lower Cooling Plate	41
14	Bottom Side of Lower Cooling Plate	41
15	General View of Equipment for Spherical Chamber Tests	42
16	One Inch Diameter Spherical Chamber	42
17	Typical Pressure vs. Time Records	52
18	Reaction Rate vs. Temperature, Isothermal Heating	53
19	Initial Rate of Pressure Decrease vs. Hot Plate Temperature, Gradient Heating	54

LIST OF FIGURES (continued)

Figure No.	Title	Page
20	Junction of the First and Second Explosion Limits, Temperature = 1490°R	55
21	Junction of the First and Second Explosion Limits, Temperature = 1440°R	56
22	Typical Temperature Profiles Along the Top Plate, Gradient Heating	57
23	Temperature Distribution Between the Plates	58

I. INTRODUCTION

A great deal of experimental work and considerable thought have been directed at determining the detailed mechanism of the chemical reaction between hydrogen and oxygen (1, 2). Experiments have been conducted over a wide range of pressures and temperatures. Configuration, size, and surface characteristics of the reaction chamber have been varied. From this work it has been possible to deduce a quite detailed mechanism by which the reaction proceeds. This mechanism accounts for the behavior of hydrogen-oxygen mixtures under a wide variety of conditions. A description of this accepted reaction scheme is given together with a discussion of its application to the present investigation in part II.

Experiments with hydrogen and oxygen have primarily been directed at the measurement of either the rate at which the reaction proceeds in a particular controlled environment, or the conditions under which a marked change in the nature of the reaction, e.g. an explosion, occurs. Figure 1 presents a curve delineating regions in which a spontaneous explosion occurs from those in which a controlled reaction takes place. This curve is shown as a function of temperature and pressure for a stoichiometric mixture of hydrogen and oxygen. Three distinct boundaries are apparent and are designated as the first, second, and third explosion limits, respectively, beginning with the one which occurs at the lowest pressure. It should be noted that the values of temperature and pressure which determine

Figure 1

Explosion Limits for a Stoichiometric Hydrogen-Oxygen Mixture
Vessel Diameter 2.9 inches KCl coating
Replotted from Reference (6)

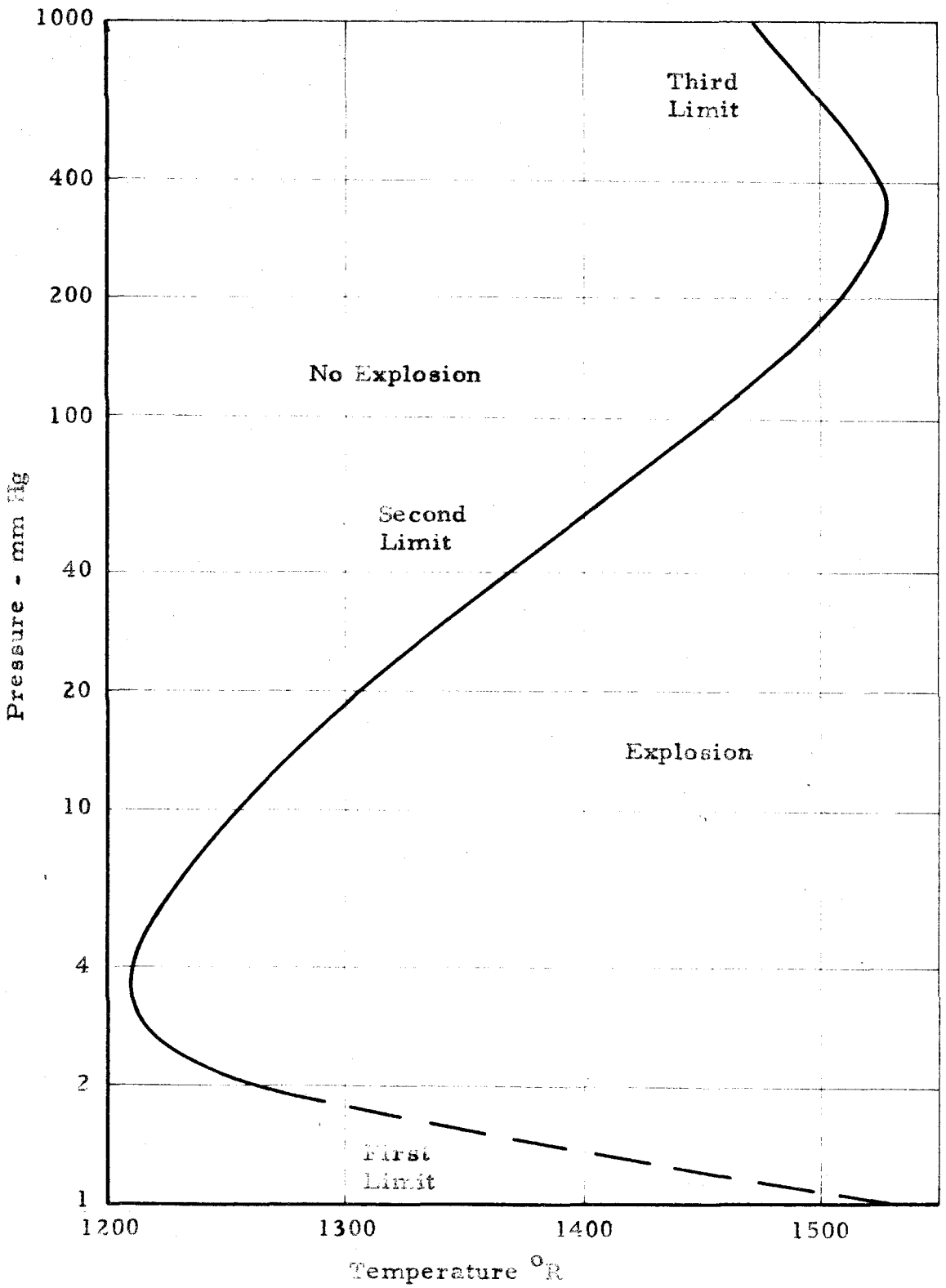

these explosion limits are dependent upon the surface characteristics, size, and configuration of the reaction vessel.

Both theoretical work and experimental data normally consider the case of isothermal conditions. This restriction is necessary in order to simplify the problem of determining the basic mechanism of a given reaction. However, this condition does not necessarily obtain in engineering applications. Experience has shown that metal surfaces can be heated, in an explosive atmosphere, to a temperature far in excess of that at which the gases would explode if heated isothermally. This observation raised a question concerning whether this behavior was caused by the temperature gradient or by some other effect. In order to study this question, an investigation was initiated in 1948.

The first part of this investigation was completed in 1950 by Glen Schurman (3). He studied the reaction of a stoichiometric mixture of hydrogen and oxygen in a chamber designed for applying a strong temperature gradient to the gases. This chamber consisted of two flat metal plates twelve inches square separated by one-half inch and closed on the sides by thin metal walls. The top plate was heated and the bottom plate kept at approximately room temperature by cooling water. In this manner a temperature gradient of as high as $2000^{\circ}F$ per inch could be maintained. The chamber was vented to the atmosphere and the reacting gases introduced between the plates at a low flow rate until equilibrium was established. Then

the flow was shut off and photographs were taken of the interference fringes produced by the mixture, with the chamber located in one leg of a Mach-Zehnder interferometer. A hydrogen-oxygen mixture was chosen for this investigation as a compromise between the use of hydrocarbon fuels, whose oxidation reactions are only incompletely understood, and the selection of one of the many well understood but not commonly used reaction systems.

Schurman's investigation definitely established the following facts:

1. The stoichiometric mixture of hydrogen and oxygen failed to explode spontaneously when the top plate was as hot as 1710°R.
2. The mixture could be made to explode by a sharp pulse of gas as late as three minutes after the flow had been shut off with top plate temperatures above 1560°R.
3. A concentration gradient existed in the mixture near the top plate at temperatures between 1500°R and 1540°R for at least nine seconds after the flow had been shut off. This persistence of a concentration gradient was inconsistent with diffusion calculations unless the reaction was proceeding at such a rate that the reactants would have been completely consumed in less than one minute. However, the

consumption of reactants in this short a time was ruled out by the explosion observation noted above.

Because of limitations in the existing equipment it was impossible for Schurman to establish definitely the causes of the phenomenon which he observed. He did, however, suggest several possible causes which formed the starting point for the present investigation.

The objectives of the present work were to establish definitely the causes of the behavior of the hydrogen-oxygen system in a temperature gradient and possibly to extend this work to various hydrocarbon systems. Because much had been learned about the nature of the system since the original equipment was conceived, it was decided to build an entirely new combustion chamber and to employ somewhat different instrumentation.

To begin with, it was necessary to determine the mixture composition in the original chamber as a function of position and time. The interferometer used by Schurman was limited by the fact that it could not, by its nature, distinguish between a change in composition and anything else which might change the index of refraction of the mixture. Consequently, a quartz prism spectrometer was designed and built with characteristics suitable for directly measuring both water and hydrogen peroxide concentration within the chamber. The determination of hydrogen peroxide concentrations was of interest since the most likely explanation of

Schurman's observations would, if correct, give rise to unusually large concentrations of this intermediate product. Preliminary investigations with the spectrometer, however, indicated that no hydrogen peroxide was present under the conditions of Schurman's experiment. In addition, it was found that hydrogen peroxide vapor introduced into the chamber decomposed extremely rapidly on the metal surfaces, even at room temperature. Investigations of this nature were then halted and a new combustion chamber designed in which it would be easier to establish the basic characteristics of the reaction in a temperature gradient.

II. PREDICTION OF REACTION RATES

Mechanism of the hydrogen-oxygen reaction

The details of the reaction between hydrogen and oxygen have been fairly well established from many thorough studies. In general, water is formed, not by simple combination of the reactants but, rather, through a series of intermediate steps. Some of the intermediate steps produce very active atoms or so-called free radicals which, due to their activity, tend to multiply in number and cause explosion of the mixture. Complex reactions which proceed by this type of mechanism are generally termed chain reactions. A good elementary discussion of complex reactions and the method of analyzing their behavior can be found in reference (4).

The most striking experimental fact which must be explained by any mechanism describing the hydrogen-oxygen reaction is the existence of three distinct explosion limits (figure 1). For the moderate pressures where the second limit is observed, the following reactions predominate:

$$OH + H_2 = H_2O + H \qquad \text{I}$$

$$H + O_2 = OH + O \qquad \text{II}$$

$$O + H_2 = OH + H \qquad \text{III}$$

$$H + O_2 + M = HO_2 + M \qquad \text{VI}$$

$$HO_2 \xrightarrow{\text{Wall}} \text{Destruction} \qquad \text{XII}$$

The numbers assigned to these equations are those usually associated with them in the literature. Reactions II and III are called chain branching reactions because they cause an increase in the number of free radicals which, if not counteracted would result in explosion. Equation VI, on the other hand, destroys the chain carrier, H, if the molecule HO_2 is assumed to be stable and unreactive enough to diffuse to the walls and there be destroyed as indicated by reaction XII. The molecule, M, appearing in reaction VI is to be interpreted as any third body, such as H_2, O_2, or H_2O, with which the hydrogen atom and the oxygen molecule collide. Each of these species may have different degrees of effectiveness in promoting reaction VI. In fact, it has been shown that water is about fourteen times as effective as hydrogen and forty times as effective as oxygen. This fact explains the high degree of sensitivity which the overall reaction shows to small changes in the concentration of water.

The expressions for the rate of formation of the various species are

$$\frac{d\left[H_2O\right]}{dt} = k_1 \left[H_2\right]\left[OH\right] \qquad (1)$$

$$\frac{d[H]}{dt} = k_1 [OH][H_2] - k_6 [H][O_2][M] \qquad (2)$$

$$\frac{d[OH]}{dt} = -k_1 [OH][H_2] + 2k_2 [H][O_2] \qquad (3)$$

where the brackets are used to indicate concentrations of a species and k is the rate constant for any given reaction. We have assumed that the concentration of oxygen atoms has reached a steady state. The factor of two in equation (3) comes from the fact that, with this assumption, the oxygen atom formed in reaction II has no choice but to react with hydrogen in reaction III, and hence, every time II occurs two OH radicals are formed.

These differential equations are typical of those found for chain reaction mechanisms and cannot, in general, be combined to yield any simple exact solution. Conventionally, a solution is obtained by making the approximation that the concentration of any free radical in the system rapidly builds up to a value which remains constant in time. For the above simple scheme, this amounts to saying that for any given concentration of hydrogen, the rate of formation of water is proportional to the concentration of the radical OH. Furthermore, setting equations (2) and (3) to zero in accordance with the above assumption and adding them yields the condition:

$$k_6 [M] = 2k_2 \qquad (4)$$

Equation (4) is an analytic expression for the boundary between a region in which the rate of water formation has a decreasing value with time and a region where water is formed at a rapidly increasing rate. This boundary is called the second explosion limit and is defined by the condition that the rate of chain branching resulting from reaction II is equal to the rate of chain breaking in reaction VI. The location of these two regions with respect to the pressure of the reactants can be deduced readily. As the pressure is lowered, the probability of a three body collision, such as reaction VI requires, becomes much smaller with respect to the probability of the occurance of a two body collision. Hence the system passes from a region of no explosion into a region of explosive reaction as the pressure is lowered (figure 1).

Equation (4) may be rewritten in such a way that the validity of this mechanism can be tested quite easily. The term M can be written more explicitly for a mixture which contains only hydrogen and oxygen as:

$$[M] = [H_2] + a[O_2] \tag{5}$$

where the symbol a accounts for the fact that the oxygen molecule may be more or less efficient than hydrogen in promoting reaction VI when the two are present in equal concentrations. Equation (4) can then be rewritten:

$$[H_2] + a[O_2] = 2\frac{k_2}{k_6} = K \tag{6}$$

This equation indicates that the second explosion limit should appear

as a straight line, at any one temperature, if plotted in rectangular coordinates measuring the concentration of hydrogen on one axis and the concentration of oxygen on the other. This straight line relationship has been shown to exist experimentally for conditions where the simplified scheme given above would be expected to apply (figure 2). Measurements of the manner in which K, the hydrogen axis intercept of this line, varies with temperature, gives a direct value for the difference in the activation energies of reactions II and VI.

At higher pressures and temperatures an additional reaction must enter the scheme to account for the occurrence of explosion at the third limit. This reaction must be one which increases the rate of chain branching at high pressures to overcome the effects of reaction VI. A suitable choice is

$$H_2 + HO_2 = H_2O_2 + H \qquad \text{XI}$$

The third limit, then, can be explained as follows. As the pressure rises, the radical HO_2 has an increasingly difficult time diffusing to the walls to complete the destruction of the chain carrier, H, initiated in reaction VI. Instead, it begins to react appreciably with hydrogen in the gas phase according to reaction XI and thereby regenerates the hydrogen atom and causes explosion.

It is possible to carry out an analysis of the reaction scheme with this new step added, in exactly the same manner as before. The result of this calculation is the addition of a term to the right hand

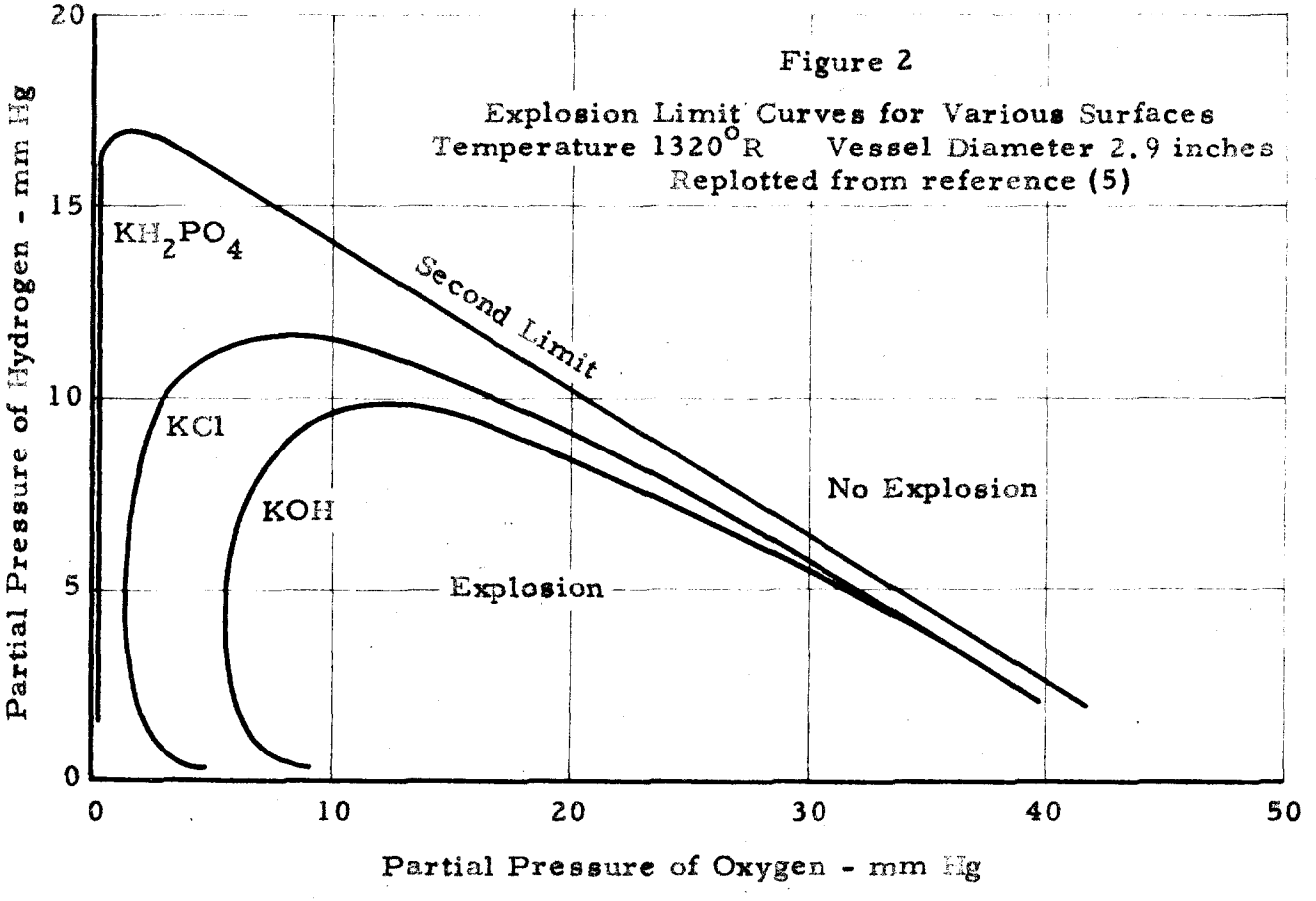

Figure 2

Explosion Limit Curves for Various Surfaces
Temperature 1320°R Vessel Diameter 2.9 inches
Replotted from reference (5)

side of equation (6) corresponding to the chain branching of reaction XI. An equation from reference (5) describing the complete range of observable explosion limits can be written:

$$[H_2] + a[O_2] + \frac{b}{[O_2]\{[H_2] + E[O_2]\}} + \frac{c}{[H_2]\{[H_2] + F[O_2]\}} = K + m[H_2]\{[H_2] + G[O_2]\} + \ell[O_2]^{-1/2} \qquad (7)$$

The terms are grouped so that those resulting from chain breaking reactions appear on the left and those which come from branching reactions are on the right. The first term on the left and the K appearing on the right constitute the basic straight line derived above. The second term on the left accounts for the destruction of oxygen atoms and OH radicals at the surface. It can be seen that this term predominates for very low concentrations of oxygen and causes the basic second limit straight line to be deflected downward in this region as shown in figure 2. The third term on the left is similar to the second but concerns the surface destruction of hydrogen atoms. The term

$$m[H_2]\{[H_2] + G[O_2]\}$$

results from the addition of reaction XI to the scheme and from its nature can be seen to be important only at the relatively high pressures of the third limit. The final term comes from still another chain branching reaction which is found to occur only in vessels with certain surface characteristics.

The presentation of an expression for the explosion limits in the form of equation (7) has two evident advantages. It simplifies the interpretation of experimental data in terms of the basic processes, and it indicates the regions in which experimentation will be most likely to yield unambiguous results.

Another presentation of this same type of analysis, which, however, describes not only the explosion limits but also the rate of the steady state reaction occurring between the second and third limits, is given by Lewis and von Elbe in reference (1). In addition to the basic reactions already presented, these authors add the following reactions to describe their observations:

$$H_2O_2 + M = 2OH + M \qquad i$$

$$HO_2 + H_2O_2 = H_2O + O_2 + OH \qquad VII$$

$$H_2O_2 \xrightarrow{\text{wall}} H_2O + \frac{1}{2} O_2 \qquad XIII$$

$$H_2 + O_2 \xrightarrow{\text{wall}} H_2O_2 \qquad XIV$$

They derive an expression for the rate of water formation by assuming that all of the free radicals and hydrogen peroxide attain a steady state concentration, just as was done in the simple example above. The rate equation obtained, as well as the numerical values which were found to best fit the experimental data for vessels coated with potassium chloride, are given below.

$$R = \frac{d\left[H_2O\right]}{dt} = 2Ix \left[1 + \frac{1}{2} u + \frac{a(1+x+b)(1+cx) + 2x}{1 - a(1+x+b)} \right] \qquad (8)$$

where x is found from the cubic equation:

$$ac\,x^3 + \left[2 + a\left\{c(1+b) - (1+u)\right\}\right] x^2 + \left[a\left\{s - (1+u)(1+b)\right\} + (1+u) - (1+2b)\right] x + sa(1+b) - s = 0 \qquad (9)$$

and

$$a = \frac{2k_2}{k_6[M]} = \frac{0.0556}{f_{H_2} + 0.35 f_{O_2} + 14.3 f_{H_2O}} \cdot \frac{T}{p} \, e^{-\left[\frac{17000}{803\,R}\left(\frac{803}{T} - 1\right)\right]} \qquad (10)$$

$$b = \frac{k_{11}[H_2]}{k_6[M]} = 0.0232 \left(\frac{pd}{T}\right)^2 f_{H_2}\left(f_{H_2} + 6.88 f_{O_2} + 7.84 f_{N_2}\right) e^{-\left[\frac{24000}{803\,R}\left(\frac{803}{T} - 1\right)\right]} \qquad (11)$$

$$c = \frac{k_5 K_{12}}{k_7 k_2} = \frac{6.03}{f_{H_2} + 6.88 f_{O_2} + 7.84 f_{N_2}} \cdot \frac{T}{pd^2} \, e^{+\left[\frac{31000}{803\,R}\left(\frac{803}{T} - 1\right)\right]} \qquad (12)$$

$$I = \frac{k_i[M]K_{12}}{k_7} = 6.36 \times 10^{-4} \, \frac{T^{3/2}}{d^2} \, \frac{f_{H_2} + 0.414 f_{O_2} + 0.454 f_{N_2}}{f_{H_2} + 6.88 f_{O_2} + 7.84 f_{N_2}} \times e^{-\left[\frac{31500}{803\,R}\left(\frac{803}{T} - 1\right)\right]} \text{ mm Hg/min} \qquad (13)$$

$$u = \frac{K_{13}}{k_i[M]} = 3.12 \, \frac{T}{pd} \, \frac{1}{f_{H_2} + 0.414 f_{O_2} + 0.454 f_{N_2}} \, e^{+\left[\frac{33800}{803\,R}\left(\frac{803}{T} - 1\right)\right]} \qquad (14)$$

$$s = \frac{k_7 K_{14}}{k_i [M] K_{12}}$$

$$= 4.26 \times 10^{-3} d \frac{f_{H_2} + 6.88 f_{O_2} + 7.84 f_{N_2}}{f_{H_2} + 0.414 f_{O_2} + 0.454 f_{N_2}} e^{+\left[\frac{27700}{803 R}\left(\frac{803}{T} - 1\right)\right]} \quad (15)$$

$$x = \frac{k_7 [H_2O_2]}{K_{12}} \quad (16)$$

These equations are expressed in terms of the absolute temperature, T, in ^{o}K., the pressure, p, in mm Hg, mixture composition in terms of mole fraction, f, and vessel diameter, d, in centimeters. R is the universal gas constant in calories per degree. The symbol k represents the rate constant for a given reaction. A capital K indicates that the mechanism of the reaction is not completely understood and therefore all of the rate determining variables have been lumped into this one constant.

The above equations represent a very good quantitative description of the behavior of hydrogen-oxygen mixtures in spherical vessels coated with potassium chloride. They were used as a starting point in the analysis of the results of the present investigation. Reaction rates and the explosion conditions were calculated from these equations for a wide variety of temperatures, pressures, vessel diameters, and mixture compositions. Figures 3 and 4 present some of the results of these calculations.

These computations were greatly speeded by the use of an

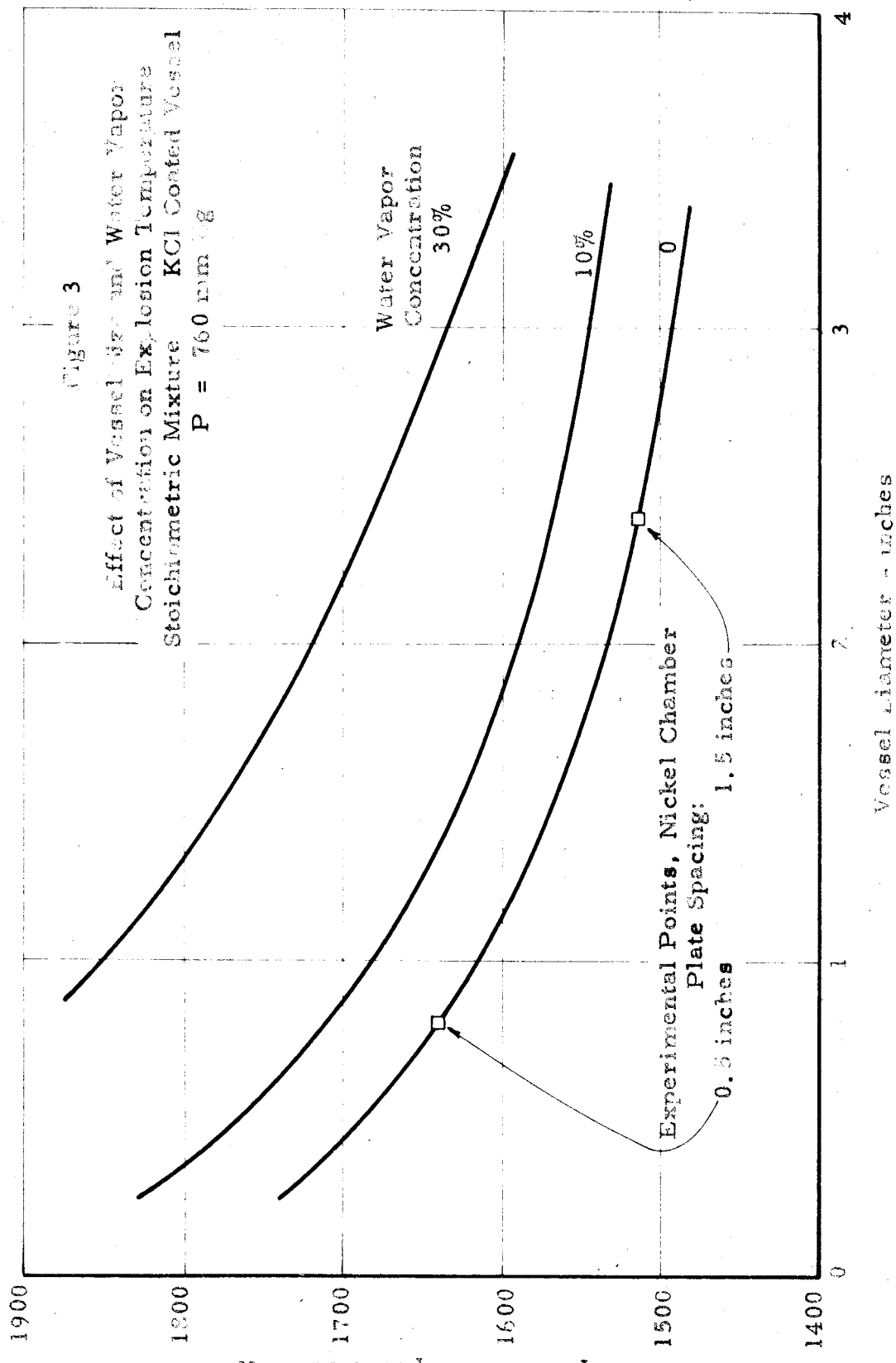
Figure 3
Effect of Vessel Size and Water Vapor Concentration on Explosion Temperature
Stoichiometric Mixture KCl Coated Vessel
P = 760 mm Hg
Water Vapor Concentration
30%
10%
0
Experimental Points, Nickel Chamber
Plate Spacing:
0.5 inches
1.5 inches
Explosion Temperature - °R
Vessel Diameter - inches
1900
1800
1700
1600
1500
1400
0
1
2
3
4

Figure 4

Effect of Water Vapor on the Reaction Rate

Stoichiometric Mixture — Vessel Diameter 3 inches

Pressure 760 mm Hg — KCl Coating

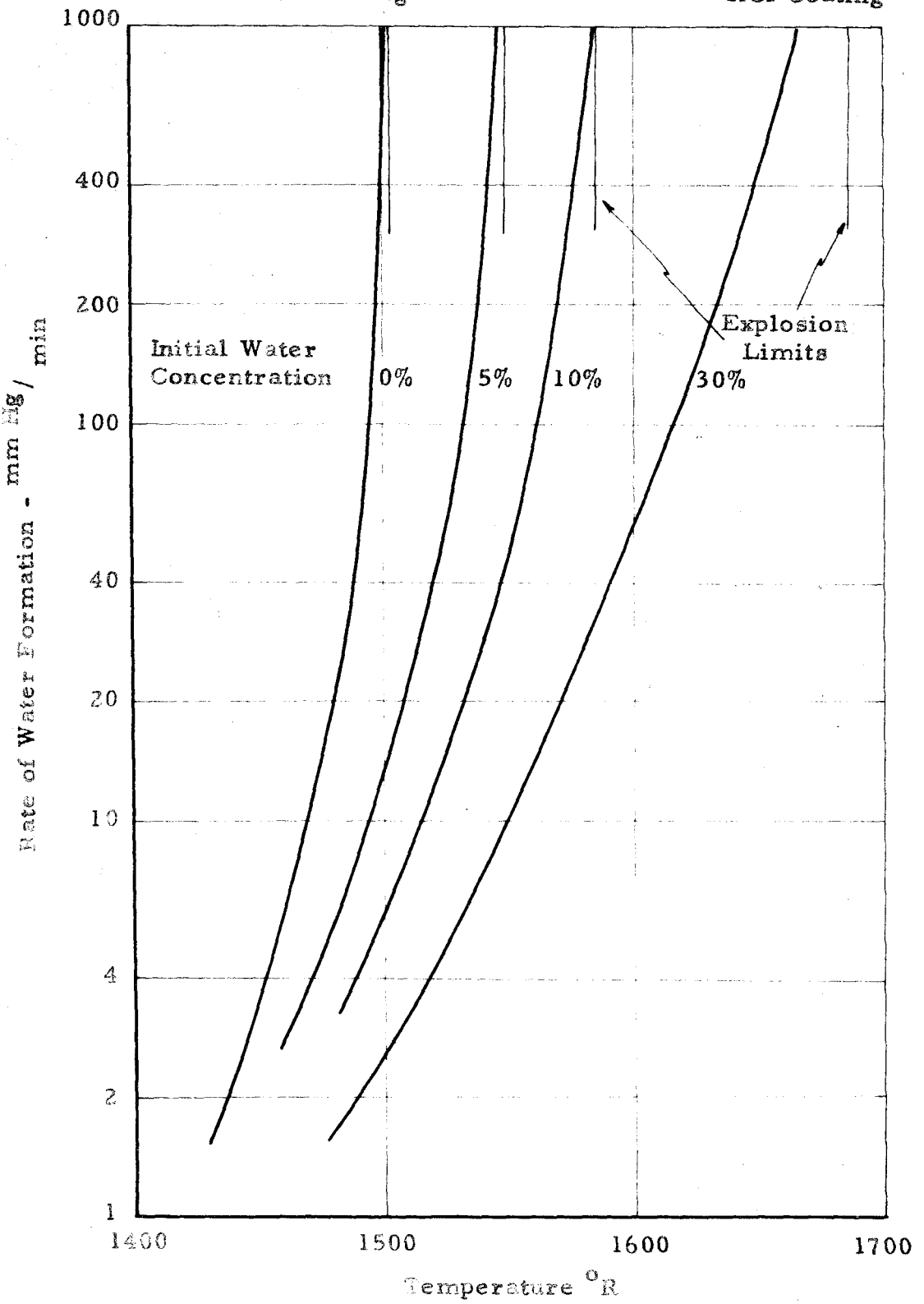

IBM type 604 calculating punch. Though the type 604 is not elegant among current computing machines, it was found that with the use of approximately ten different control panels, this machine was perfectly adequate for the present calculations. The most obvious saving of time occurred in the solution of the cubic equation (9), which was accomplished by an iterative process. The availability of this computer was what made possible the investigation of the above equations for such a wide range of variables in a reasonable length of time.

Effect of chamber geometry and surface characteristics

In any effort to compare new data on the rate of water formation with the results of previous investigators, it is necessary to account for the differences in experimental conditions. The most important differences to be considered in the present case are the effect of a different chamber geometry and the change in surface characteristics.

Fortunately, it is possible to separate, experimentally, the effects of a change in chamber geometry and a change in surface type. The explosion condition is determined by the relative rates of chain branching and chain destruction in the system as is shown above by equation (7). It can be shown that it is relatively independent of the surface characteristics as long as the chain destructiveness of the surface is high (6).

On the other hand, the rate of the reaction at very low

temperatures is dependent entirely upon the surface characteristics. Upon examination of the reaction scheme given above it becomes evident that at very low temperatures the rate expression, equation (8), reduces to

$$R = Is = K_{14}$$

This simplification is caused analytically by the exponential factors which make the terms a and b much smaller than the terms c, s, and u at low temperatures. Physically this simplification results since few of the reactant molecules at low temperatures possess sufficient energy to participate in the gas phase reactions. K_{14}, it will be recalled, is the rate of the surface catalytic reaction between hydrogen and oxygen. Furthermore, it can be shown that the value of K_{14} has no effect on the conditions for explosion, with the reaction scheme given above, which simplifies the task of comparing reaction chamber configurations.

The effect of the chamber geometry arises from two sources:

1. Since the reaction between hydrogen and oxygen is heterogeneous, the relationship between the surface area and the enclosed volume of the chamber is important.
2. Most of the active particle chain carriers which continue the gas phase reaction and cause explosion can be destroyed upon contact with the wall. Since

the rate of destruction of these chain carriers is dependent upon the average distance that they must diffuse to a surface, the chamber geometry has, in this manner, a definite influence on the gas phase reaction.

The problem of analyzing the average chain carrier concentration in enclosures of various configurations has been previously treated (7). The ideal case of a chamber consisting of two infinite parallel planes, and having surfaces which are almost certain to destroy a chain carrier upon collision, is presented below.

The general equation describing the steady state concentration of chain carriers in a system such as this is

$$D \frac{d^2 n}{dx^2} + \alpha n + n_o = 0 \qquad (17)$$

where n = the concentration of the chain carrier in various parts of the vessel,

x = the coordinate describing the position of a plane between and parallel to the boundaries,

D = the diffusion coefficient of the chain carrier through the mixture, assumed to be constant,

αn = net rate of chain branching per unit volume from chemical reaction in the mixture,

n_o = rate of chain initiation per unit volume,

and the boundary conditions can be written:

$$n(o) = 0 ; \quad \frac{dn}{dx}_{\ell/2} = 0 \tag{18}$$

where ℓ = the distance between the parallel planes. The solution of the above problem can be written by conventional methods as follows:

$$n = \frac{n_o}{\alpha} \left[\frac{\cos \sqrt{\frac{\alpha}{D}}\, x}{\cos \sqrt{\frac{\alpha}{D}}\, \frac{\ell}{2}} - 1 \right] \tag{19}$$

The average concentration of the chain carrier within the vessel is then

$$\bar{n} = \frac{2}{\ell} \int_o^{\ell/2} n(x)\, dx \tag{20}$$

$$\bar{n} = \frac{n_o}{\alpha} \left[\frac{\mathrm{Tan} \sqrt{\frac{\alpha}{D}}\, \frac{\ell}{2}}{\sqrt{\frac{\alpha}{D}}\, \frac{\ell}{2}} - 1 \right] \tag{21}$$

Now

$$\mathrm{Tan}\, x = \sum_{n=1}^{\infty} \frac{8x}{(2n-1)^2 \pi^2 - 4x^2}$$

and therefore we can write

$$\bar{n} = \frac{n_o}{\alpha} \left[\left\{ \sum_{n=1}^{\infty} \frac{8}{(2n-1)^2 \pi^2 - \frac{}{D}^2} \right\} - 1 \right] . \tag{22}$$

A similar solution for the case of a spherical chamber is outlined below:

$$D \frac{1}{r^2} \frac{d}{dr} \left(r^2 \frac{dn}{dr} \right) + \alpha n + n_o = 0 \tag{23}$$

with boundary conditions:

$$n(r_o) = 0 \; ; \quad n(o) = \text{finite} \tag{24}$$

then

$$n = \frac{n_o}{\alpha} \left[\frac{r_o}{r} \frac{\sin \sqrt{\frac{\alpha}{D}}\, r}{\sin \sqrt{\frac{\alpha}{D}}\, r_o} - 1 \right] \tag{25}$$

and

$$\bar{n} = \frac{n_o}{\alpha} \left[3 \left\{ \frac{1}{r_o^2 \frac{\alpha}{D}} - \frac{\operatorname{Cot} \sqrt{\frac{\alpha}{D}}\, r_o}{\sqrt{\frac{\alpha}{D}}\, r_o} \right\} - 1 \right] \tag{26}$$

Now:

$$\operatorname{Cot} x = \frac{1}{x} - \sum_{n=1}^{\infty} \frac{2x}{n^2 \pi^2 - x^2} \tag{27}$$

and therefore we can write

$$\bar{n} = \frac{n_o}{\alpha} \left[\left\{ \sum_{n=1}^{\infty} \frac{6}{n^2 \pi^2 - \frac{\alpha}{D} r_o^2} \right\} - 1 \right] \tag{28}$$

We should like to compare these two cases near the point where explosion is imminent, i.e. where the average concentration of chain carriers, $\bar{n}$, becomes very large. In this region only the first term of each series is needed and equations (22) and (28) can be written, respectively:

$$\bar{n} = \frac{8\, n_o/\alpha}{\pi^2 - \frac{\alpha}{D} \ell^2} \tag{29}$$

and

$$\bar{n} = \frac{6 n_o / \alpha}{\pi^2 - \frac{\alpha}{D} r_o^2} \tag{30}$$

This result indicates that the chamber consisting of two parallel planes should exhibit the same characteristics with regard to explosion conditions as a spherical chamber having a diameter of twice the spacing between the plates.

Reaction mechanism in a temperature gradient

The most common method of measuring the rate at which a reaction proceeds is to measure the way in which the pressure of a closed system varies with time. In the case where a considerable temperature gradient is present, however, the task of relating this measured rate of pressure change to the change in number of moles in the system, must be done carefully.

Normally one considers N moles of a perfect gas at pressure p and enclosed in a volume V at an absolute temperature T so that

$$pV = NRT \tag{31}$$

where R is the universal gas constant. Then, the rate of change of the number of moles in a fixed volume at a given temperature is directly proportional to the rate of pressure decrease:

$$\frac{dN}{dt} = \left(\frac{V}{RT}\right) \frac{dp}{dt} \tag{32}$$

Equation (32) still applies to a perfect gas system in which the temperature varies from point to point if the temperature remains

independent of time. The following section concerns the details of this calculation of the average overall pressure decrease in such a system.

Consider the ideal case of a reacting gaseous chemical mixture which is confined between two infinite parallel planes in a gravity free space. The two planes are at different temperatures and hence the chemical reaction along any plane parallel to the boundaries proceeds at a rate which varies with the coordinate, x, describing the position of that plane. Because of the chemical reaction, the relative concentration, a_i, of any chemical species, that is, the mass of that species divided by the total mass of the mixture, is changing with time in every region. Diffusion will of course take place under these conditions and attempt to eliminate any concentration gradients. To describe this process, then, we may write the normal diffusion equation for each species, i, with a term added for the rate of chemical formation of that species:

$$\frac{\partial \rho a_i}{\partial t} = \frac{\partial}{\partial x}\left(D_i \rho \frac{\partial a_i}{\partial x} \right) + \Phi_i \qquad (33)$$

where ρ = the density of the mixture,

D_i = the diffusion constant of species i into the mixture,

Φ_i = the rate of formation of species i from chemical reaction.

This equation is subject to certain boundary conditions which are

determined by the rate at which each of the species are formed and/or destroyed at the surfaces. The initial conditions, in general, would specify the concentration of each species at some fixed time. The Φ_i are functions of products of the concentrations a_i, as well as the temperature and pressure. To complete the specification of this problem it would normally be necessary to write an equation which describes the energy changes taking place in the system. For the present case, however, with a strong temperature gradient, it is satisfactory to assume that the temperature profile is fixed by the temperatures of the boundaries and remains constant in time. This assumption will be valid if we treat a mixture for which the rate of heat release upon reaction is a small portion of the heat being transferred through the gas by conduction. Furthermore, it will be necessary to confine our attention to a portion of the process during which no significant change in the thermal conductivity of the mixture takes place.

This problem could be solved in a satisfactory manner if applied to a relatively simple reaction system. It would be necessary to choose a system in which the number of species is small and suitable values for the diffusion coefficients and rates of both the surface and gaseous reactions could be found. In fact, a similar problem has been solved, with regard to the flame propagation rate of several mixtures, by the use of high speed computing equipment (8). In the present case, however, this computation is very difficult because of

the large number of intermediate products which should be considered. Furthermore, the usefulness of such a calculation in this case is questionable in view of the uncertainties in the basic data used in the analysis.

In order to obtain some information about the processes occurring, we will simplify the problem greatly by treating, approximately, the two cases which result when either the diffusion process or the chemical reaction process predominates. We shall consider only the primary species, hydrogen, oxygen and water, and ignore the existence of the temperature gradient for the diffusion calculation.

Consider the case in which a very large rate of reaction is taking place near the hot surface so that nearly all of the slowest diffusing species is being consumed as rapidly as it arrives. The problem, then, reduces to that of calculating the rate at which oxygen can diffuse from the bulk of the mixture into this reacting layer. Letting

$$c = \frac{\text{concentration of oxygen at any point}}{\text{original uniform concentration of oxygen}}$$

and assuming that D is a constant, we may write

$$\frac{\partial c}{\partial t} = D \frac{\partial^2 c}{\partial x^2} \tag{34}$$

where initially: $c = c(x,o) = 1$

and at the hot surface: $c = c(o,t) = 0$

and at the cold surface: $\frac{\partial c}{\partial t} = \frac{\partial c}{\partial t}(\ell,t) = 0.$

The solution of this problem may be written:

$$c(x,t) = \frac{4}{\pi} \sum_{n=0}^{\infty} e^{-\left(\frac{2n+1}{2} \frac{\pi}{\ell}\right)^2 Dt} \frac{\sin \frac{2n+1}{2} \pi \frac{x}{\ell}}{2n+1} \qquad (35)$$

Integrating over the span between the plates, ℓ , to obtain the total relative concentration of oxygen, C , at any time, we obtain:

$$C = \frac{8}{\pi^2} \sum_{n=1,3,5..}^{\infty} \frac{1}{n^2} e^{-\left(\frac{n\pi}{2\ell}\right)^2 Dt} \qquad (36)$$

Equation (36) may be evaluated, using for the diffusion constant the rate of diffusion of oxygen into water at 100°C: 0.38 sq. cm./sec (9). This value should yield a conservative estimate of the rate at which oxygen is supplied to the upper plate. This computation indicates that, with a plate spacing of one-half inch, the oxygen concentration in the chamber is reduced to two per cent of its initial value in, roughly, 6 seconds. This corresponds to an average rate of pressure decrease of 2500 mm Hg/min, if the system is originally at atmospheric pressure, and indicates that, for all but explosive rates of reaction, the diffusion process is certainly not the slowest step.

The second extreme case assumes that the diffusion processes are rapid enough to eliminate any concentration gradients within the system. With this assumption, the overall rate of pressure decrease can be determined in the following manner. If n is the number of moles per unit area, then, from equation (31) in a small layer of gas, dx:

$$dn = \frac{p\,dx}{R\,T(x)} \quad . \tag{37}$$

Since T is assumed to be independent of time, the rate of change of the total number of moles per unit area within the system is given by:

$$\frac{dn}{dt} = \frac{1}{R}\,\frac{dp}{dt}\int_0^{\ell}\frac{dx}{T(x)} \tag{38}$$

or,

$$\frac{dp}{dt} = \frac{R\,\frac{dn}{dt}}{\int_0^{\ell}\frac{dx}{T(x)}} \tag{39}$$

The term $\frac{dn}{dt}$ can be evaluated from isothermal data only if two assumptions are made:

1. There exists no interaction between the catalytic surface reaction and the gas phase reaction.
2. The diffusion of the intermediate products formed at one temperature into the reactants in a region of different temperature has no effect on the reaction.

The validity of these assumptions will be discussed below when the experimental data of the present investigation are presented.

III. EQUIPMENT

Combustion chamber design

With the clear formulation of the problem outlined above, the need for a new combustion chamber became apparent. It had to differ from the existing chamber in meeting two basic requirements:

1. It had to be capable of isothermal as well as gradient heating in order to keep to a minimum the difficulty of establishing the existence and the cause of any unusual results in the gradient tests.
2. It had to be a closed, constant volume system in which a measurement of the overall reaction rate would be simple and no question would exist regarding contamination from the atmosphere.

Other requirements soon became apparent. Previous investigators have found that the initial reaction rate, and the explosion temperature of hydrogen-oxygen mixtures are extremely sensitive to minute amounts of water which may be formed during the time when the reactants have been introduced to the chamber and before measurements can be taken (10). From figures 3 and 4 it can be seen that reaction rates are reduced markedly and the explosion temperature is raised appreciably by as little as 5% water formation. This fact makes it extremely difficult to observe the very large initial reaction rates near the region of explosion. Inevitably, under these

conditions, an appreciable, but unknown amount of water is formed during the manipulation period which makes measurements meaningless.

Since it would be desirable to make measurements as close as possible to the temperature of explosion, for comparison with the reaction conditions in the gradient system near the hot plate, it was decided to attempt to overcome this problem at the expense of complicating the chamber design. Some means was required for suddenly imposing the explosion conditions on a fresh mixture of reactants. Fortunately, the reaction rate between hydrogen and oxygen is quite markedly dependent upon pressure as well as temperature, and it seemed much more feasible to attempt to change the pressure rapidly than the temperature. It appeared that if a mixture were introduced to the heated chamber at approximately one-half atmospheric pressure and compressed rapidly to one atmosphere, the requirements could be met. Therefore, a cylindrical combustion chamber was designed. Its diameter was chosen to be 10.75 inches in order to minimize edge effects. The bottom of the cylinder was closed by a flat plate and the upper end fitted with a piston which could be moved up and down. The distance between the two plates could be varied from 1/4 to 1-1/2 inches.

Other requirements included provisions for windows for optical measurements, and for positive protection in the case of a violent explosion. Upper and lower plates were made of copper

to reduce temperature gradients along their span. Stainless steel was used throughout the rest of the chamber for strength at high temperatures and to reduce heat transfer through the walls connecting the upper and lower plate.

Provision of an adequate seal between the chamber and the atmosphere presented a major problem, especially at the moving piston. Sealing was attempted in the following manner. The bottom copper plate was furnace brazed to the stainless steel cylinder. The upper plate was connected to a stainless steel bellows, 8 inches in diameter, which, in turn, was sealed to the cylinder at a flange joint by means of a circular 1/8 inch stainless steel "O" ring. The windows were 1-1/2 inches in diameter and were cemented into two small bellows to provide flexibility and to prevent cracking of the quartz from stresses imposed as the mounts were heated and cooled. These bellows were similarly sealed to the chamber proper with stainless steel "O" rings.

A combustion chamber was built to these specifications and put into operation. However, adequate sealing could not be achieved. It was found impossible to obtain a gas-tight furnace braze between the lower copper plate and the stainless steel cylinder with commercial brazing materials that have appreciable strength at 1750^{o}R. No commercial sealing compound or cement could be found which did not become porous after one cycle of operation between room temperature and 1750^{o}R. A complete redesign of the chamber became necessary in order to meet the basic requirements.

The chamber in its final form is shown in figures 5, 6 and 7. Its basic dimensions are the same as those of the chamber described previously. The cylinder and lower plate are machined from a single forged round of mild steel with window mounts and flanges welded on before final machining. The bore of the cylinder is finished to produce a wall thickness of 1/8 inch between the position of the upper and lower plates. The entire assembly is plated to a thickness of .001 inches with nickel by means of a chemical deposition process. Indeed, the availability of this type of plating, which produces an extremely uniform, strongly adherent layer of nickel on a metal object of virtually any shape, made this type of construction feasible. The only other alternative would have been to use stainless steel throughout the system, and this would have been intolerable from the standpoint of the very low thermal conductivity of this material ($K \approx 0.04$, cgs units). Even the substitution of mild steel ($K \approx 0.13$, cgs units) for copper ($K \approx 0.93$, cgs units) in the upper and lower plates produces much larger gradients within the plates than is desirable (figure 22).

The functions of window mounting and blowout protection are combined, as can be seen in figure 7. The quartz windows are securely clamped against a copper-clad asbestos gasket within a central ring, which is similarly clamped and sealed to a .002 inch shim stock blowout annulus. The outer edge of this annulus is clamped to the window mounting pads on the chamber with a third

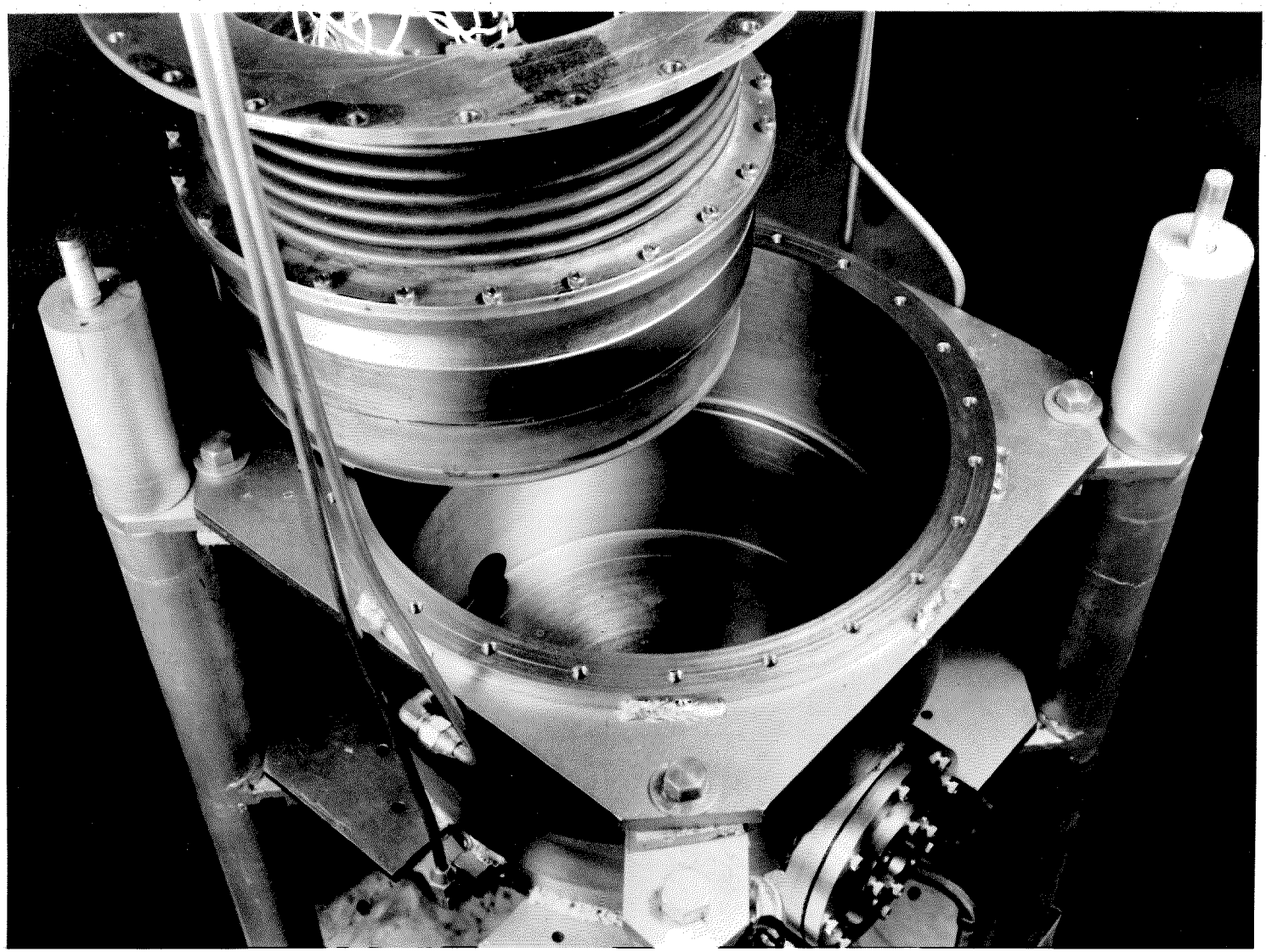

Figure 5. General View of Combustion Chamber. Inner Assembly Removed.

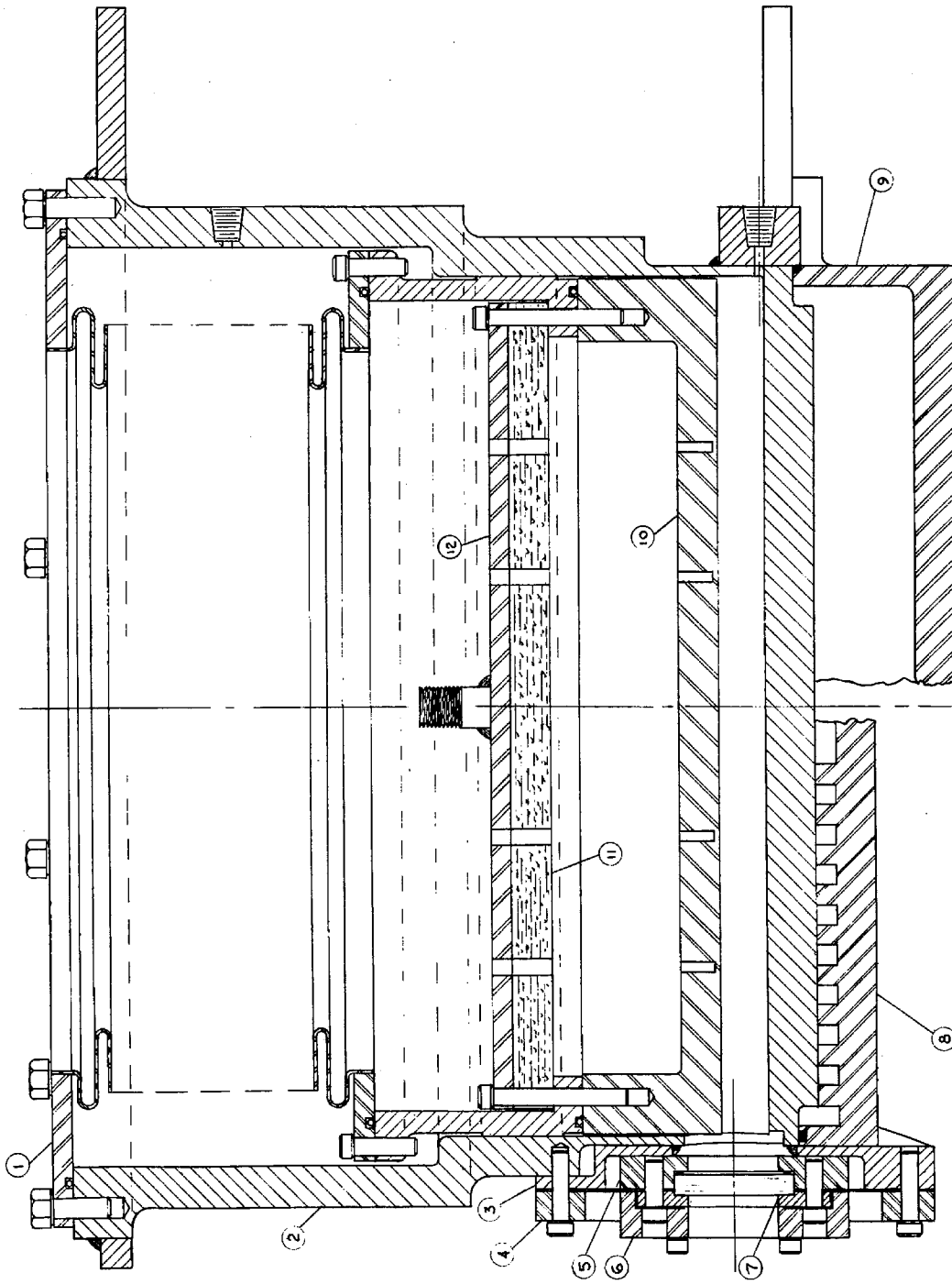

Figure 6. One-Quarter Cross-section Drawing of Chamber

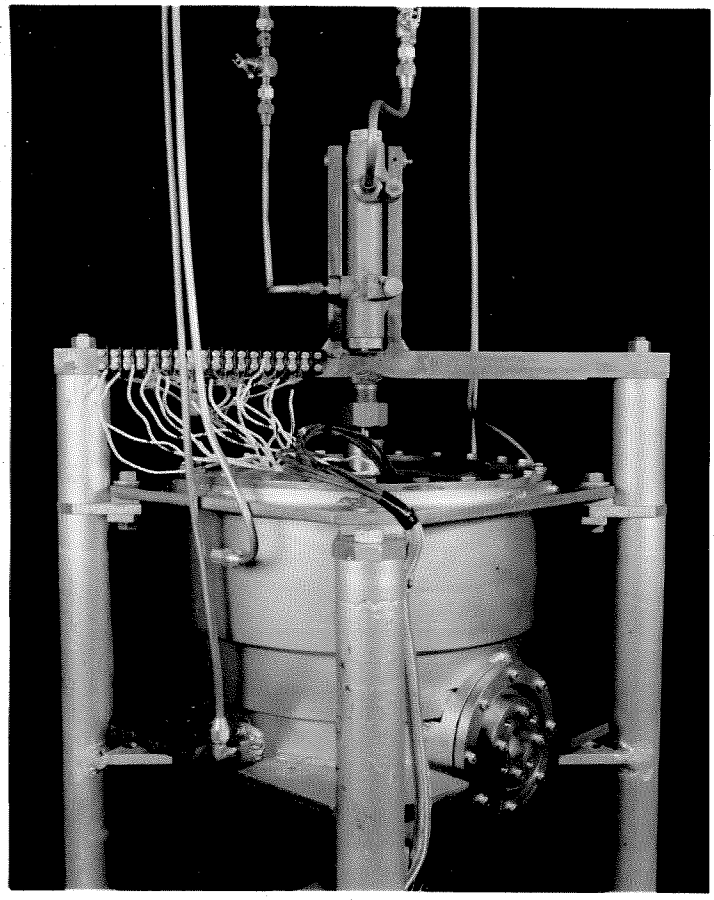

Figure 7. Outside View of Chamber

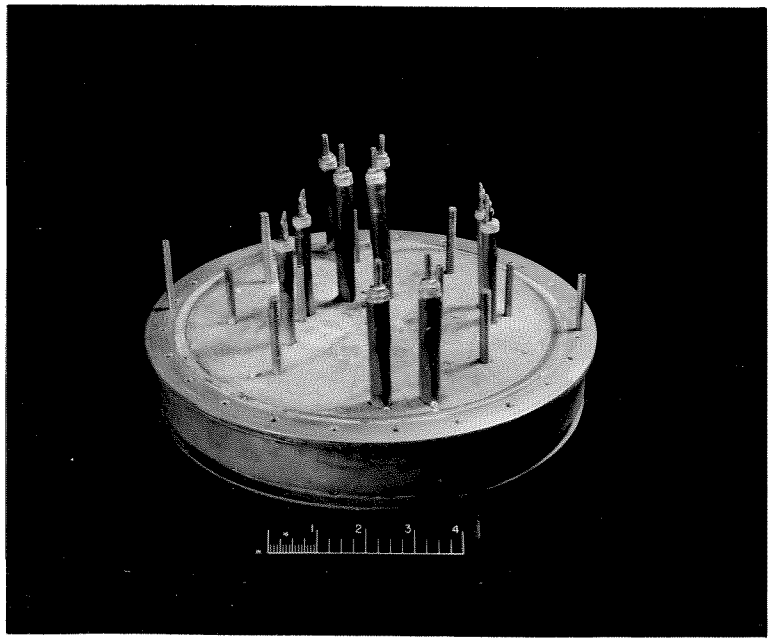

Figure 8. Upper Heating Plate

Figure 9. Heater Controls and Temperature Recorder

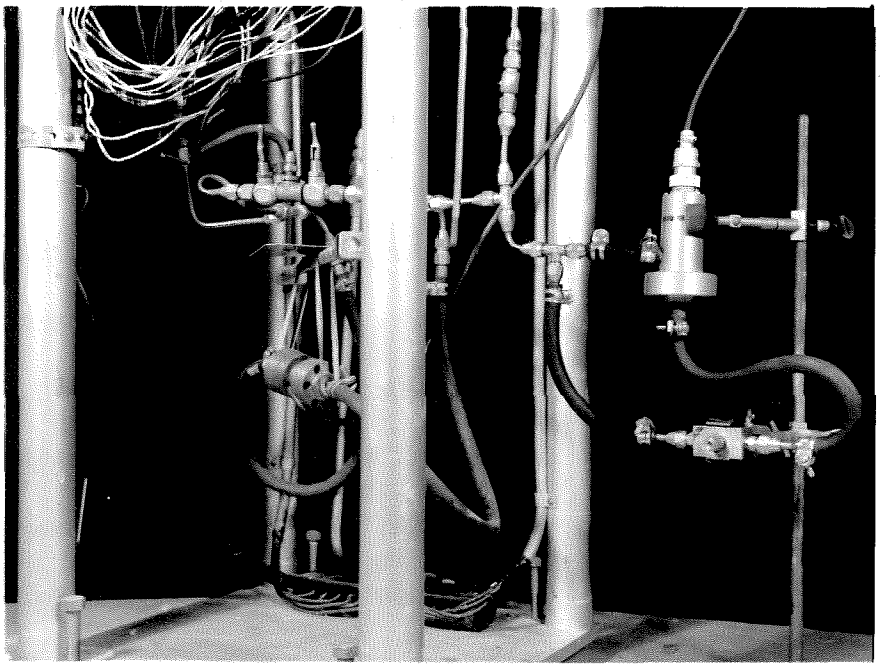

Figure 10. Pressure Transducers

copper-asbestos gasket. This shim stock supplies the required flexibility in the window mount to take care of differences in thermal expansion and, in the event of an explosion, parts near the outer clamp venting the chamber to atmosphere. Support from the mounting pads prevents the shim stock from shearing when the chamber is evacuated.

The upper plate (figure 8) consists of a shallow cylindrical dish in which five electric heating elements of 5.1 kw rated capacity are mounted and then cast in lead. The molten lead protects the individual heating elements from excessive sheath temperatures, and maintains a uniform plate temperature. Temperatures at eight different locations in the plate are measured by chromel-alumel thermocouples connected to a high speed eight-point Leeds and Northrup recording potentiometer (figure 9). These thermocouples are inserted in stainless steel protection tubes with a wall thickness of 1/64 inch, which are mounted in flat-bottom holes drilled to within 1/16 inch of the plate surface. To lessen the temperature variation across the plate, the heaters are divided into two groups and the voltage of each group is controlled by a variable autotransformer.

A 1/2 inch transite spacer and a stainless steel support plate are mounted above the lead bath. These, together with an annular ring which aligns the upper plate in the chamber, are fastened to the upper plate by means of 24 stainless steel cap screws. The joint between the annular ring and the plate is sealed by means of a

stainless steel "O" ring. A sealing bellows is similarly fastened and sealed to the alignment ring to form the complete inner assembly (figure 5). Movement of the upper plate is accomplished by means of a one inch high pressure hydraulic actuator which is mounted on the chamber support frame and attached to the stainless steel support plate.

The lower plate temperature is controlled by attaching to its outside surface, either a heating pot (figures 11 and 12) similar to the top plate, or a plate machined for the circulation of cooling water (figures 13 and 14). Rated heating capacity of the lower plate heaters is 3.7 kw. Temperature measurement and control of the heating pot are similar to that of the top plate. The heating capacity in the two lead baths is augmented by four auxiliary heaters which are clamped to the outside of the cylinder around the reaction region and two similar units located about halfway up the cylinder. These six units, whose rated capacity is 2.2 kw, are all covered with about one inch of commercial insulating cement.

The cooling plate is divided into three sections. Independent control of the water circulation rates in these sections insures the maintenance of a uniform temperature across the lower plate. Water leakage around the outer edge of the cooling plate is prevented by means of a neoprene "O" ring.

Gas can be admitted to the chamber at four locations. Two of these are 1/8 inch holes through the cylinder wall located on a line

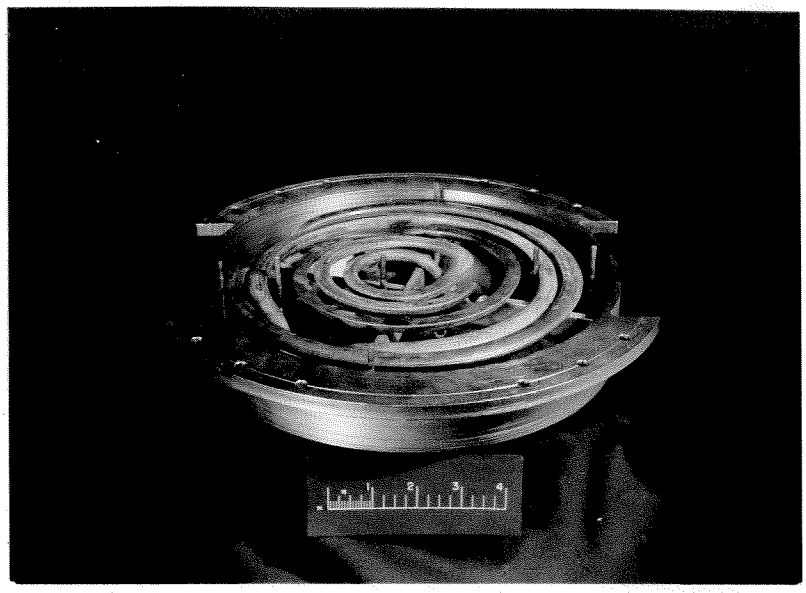

Figure 11. Top Side of Lower Heating Pot

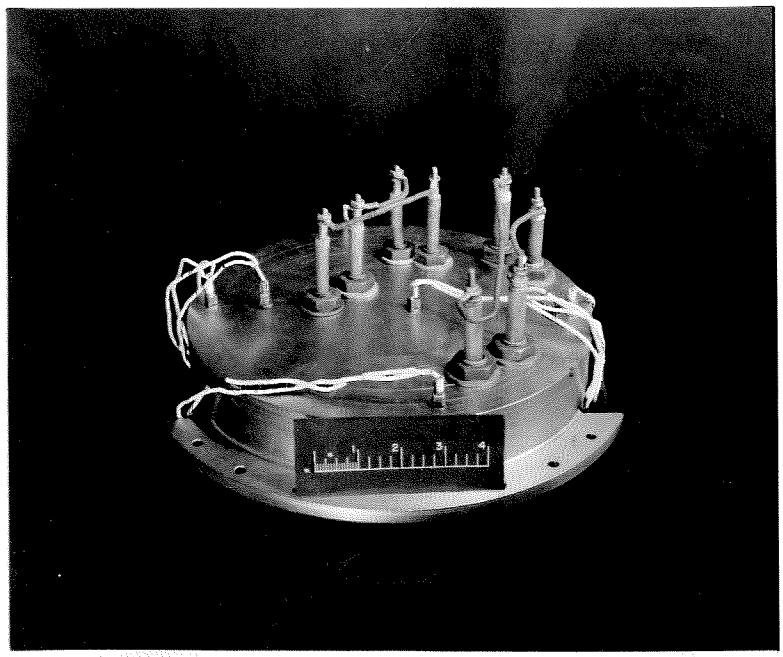

Figure 12. Bottom Side of Lower Heating Pot

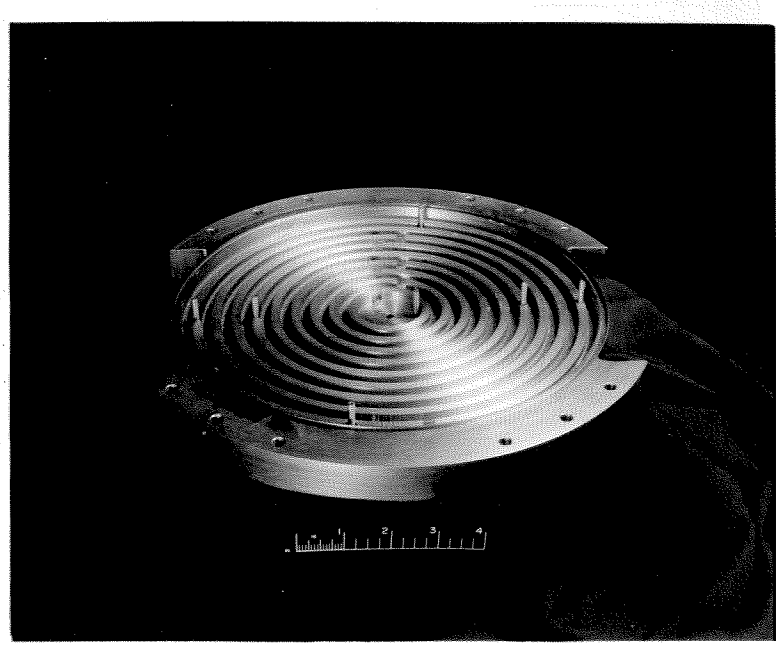

Figure 13. Top Side of Lower Cooling Plate

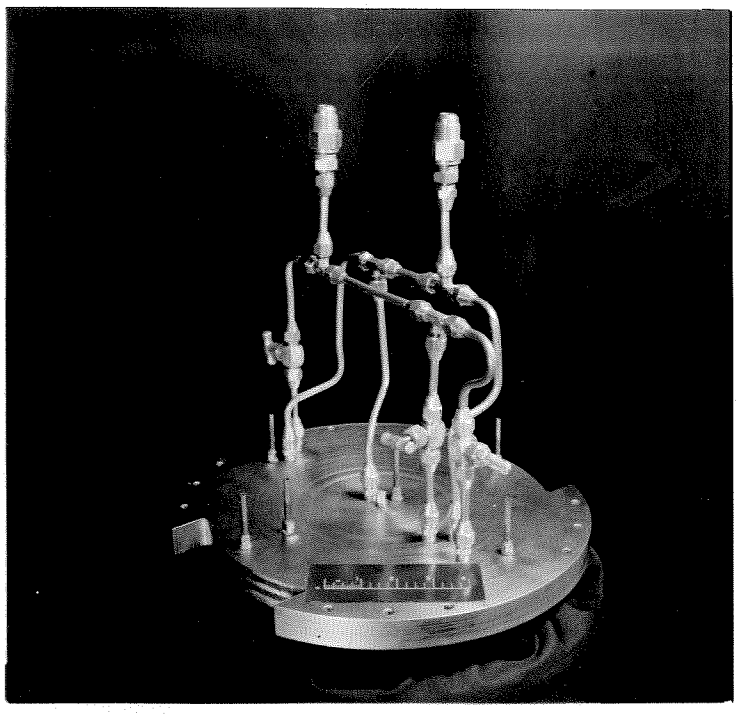

Figure 14. Bottom Side of Lower Cooling Plate

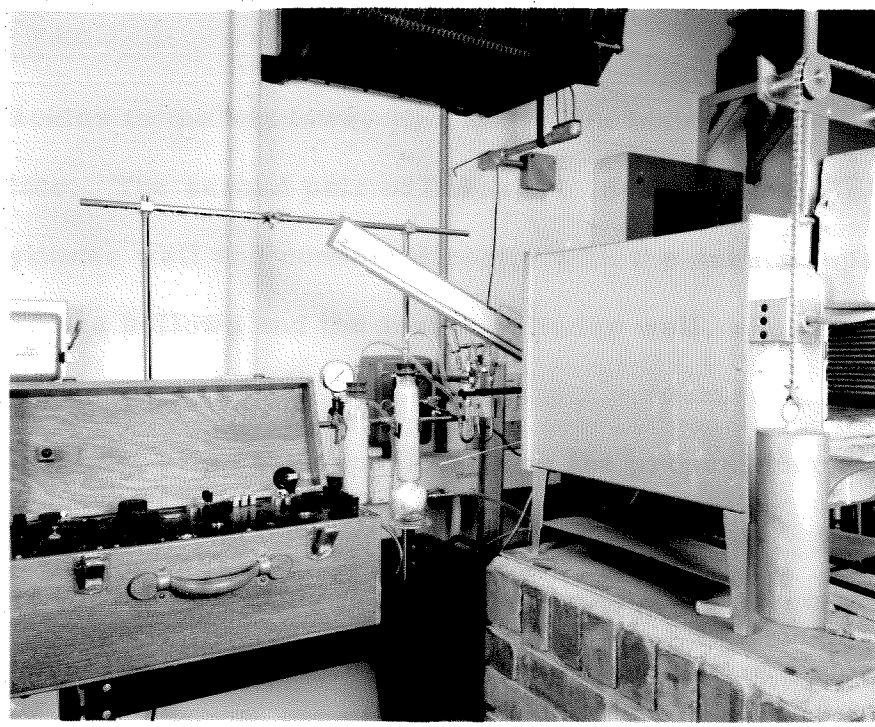

Figure 15. General View of Equipment for Spherical Chamber Tests

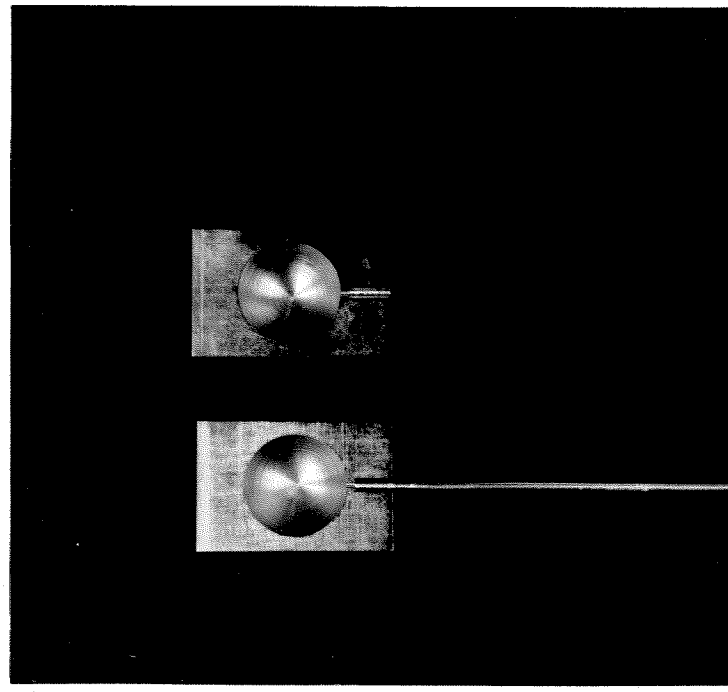

Figure 16. One Inch Diameter Spherical Chamber

perpendicular to the windows, just above the inside surface of the lower plate. The second pair of holes are located above the first in the cylinder wall and connect directly with the annular space formed by the bellows and the inside cylinder wall, above the piston alignment ring.

Almost all of the experiments in the present investigation were performed in the chamber just described. All of the surfaces in contact with the reacting mixture were plated with a coating of nickel-nickel phosphide, with a phosphorous content of about 5% resulting from the method of plating. In an effort to determine more about the chemical kinetic characteristics of this surface coating, a separate group of experiments were run in two spherical metal chambers of different diameters plated with this same material. Figure 16 shows the one inch diameter chamber before welding. A similar chamber of three inch diameter was also used.

Pressure recording system

The accurate and sensitive measurement of pressure within the combustion chamber is of primary importance since it is by this means that the reactants are metered and the overall reaction rate measured. Two differential unbonded strain gage type transducers (figure 10) and one mercury manometer are used. The recording system consists of a carrier type amplifier with integral calibration system and a direct writing oscillograph wired in parallel with an indicating meter. Maximum sensitivity is 0.1% of the range of either

transducer. Recording speeds can be 1, 5, or 25 cm/sec, and timing traces can be applied to the recorder simultaneously with the pressure signal. The overall frequency response of the system is more than adequate to record the rates encountered.

The 25 psi transducer is connected with suitable valving so that it can measure either gage pressure within the chamber at a point above or below the upper plate alignment ring, or the differential pressure between these two points. Leakage of combustible mixture past the piston seal is prevented by admitting dry nitrogen to the volume above the alignment ring. This flow is controlled by the pressure measurement mentioned above, so that a pressure differential of less than 0.05 psi across the alignment ring is maintained. Since clearance between the alignment ring and the cylinder is approximately 0.002 inches and the time of piston travel of the order of 2 seconds, negligible flow across the ring results.

The initial rate of reaction is usually recorded with the 0.7 psi transducer, designed to measure differential pressures. The reaction chamber pressure is normally applied to both pressure inlets, with an open valve in one connecting line. This arrangement permits evacuation of the chamber without overloading the transducer. Furthermore, sensitive rates of pressure change can be measured at any absolute pressure level simply by closing the valve.

The total volume of the pressure transducers and their connecting tubing, which effectively reduces the sensitivity of the chamber

pressure measurement, is approximately 5% of the chamber volume occupied by the reactants.

IV. TEST PROCEDURE

Rate determination

After assembly, the necessary checks and adjustments on the equipment were made. Rate determinations were then made in the following manner:

1. The top plate was moved to its uppermost position and the entire chamber evacuated. Then the space below the upper plate was filled with hydrogen to atmospheric pressure while the space above the alignment ring was filled with nitrogen.
2. The chamber was then heated to the required temperature while hydrogen flowed between the plates. The hot hydrogen was bubbled through water before being exhausted to the atmosphere. After temperature equilibrium had been obtained, the chamber was evacuated and fresh hydrogen admitted for the test.
3. Hydrogen was withdrawn from the chamber and then oxygen admitted so that the desired composition was obtained at approximately one-half atmospheric pressure.
4. The upper plate was next moved down so that the plate separation became 1/2 inch and the chamber

pressure nearly atmospheric. The pressure recording system was placed in operation immediately.

All of the gases used were more than 98% pure and were dried over $CaSO_4$ to remove any water. During all manipulations a balance of pressure across the alignment ring was maintained to avoid contamination of the reaction chamber with nitrogen. Analysis of the gas contained in the reaction chamber after using this procedure indicated less than 2% contamination.

Results from tests run as described above were not reproducible and did not show a consistent dependence upon temperature, particularly at temperatures above 1400°R. Subsequent tests at various plate spacings revealed that this was caused by very high rates of water formation and consequent inhibition of the reaction. This high rate was not appreciably reduced even by the low pressures maintained during the manipulation period. This observation can be explained by the fact that, since the reaction rate is a function of vessel size as well as pressure, the rate with a large plate spacing and lowered pressure might be the same as the rate existing after the mixture is compressed to atmospheric pressure by movement of the upper plate. Consequently, tests involving piston motion were abandoned and efforts made to shorten the oxygen admission time as much as possible.

The rate determinations which are reported here were made

with a fixed plate separation of 0.500 ± .003 inches. The mixture ratio was stoichiometric and the initial total pressure of the reactants 748 ± 3 mm Hg. It was necessary to purge the system with hydrogen for at least ten minutes between runs to obtain reproducible results. Oxygen admission time was approximately three seconds, and another five seconds generally elapsed before rate measurements could be taken. Adjustment of the recording equipment was made so that satisfactory rate determinations resulted in a time interval during which a pressure decrease of less than 5 mm Hg took place. This pressure decrease corresponds to a water concentration of approximately 2%.

Rate determinations with gradient heating were made in exactly the same manner as with isothermal heating. The temperature of the lower plate was maintained as high as possible with the water cooling system, 680 ± 5°R, to eliminate water condensation within the chamber.

Sampling tests

An effort was made to determine the mixture composition in the chamber after the pressure measurements indicated completion of the reaction. This was accomplished by withdrawing the contents of the chamber through a liquid nitrogen trap and analyzing the gas obtained for hydrogen and oxygen. The contents of the liquid nitrogen trap were subsequently weighed and a titration performed to determine the amount of hydrogen peroxide present. These tests

were performed at a number of temperatures with both isothermal and gradient heating.

Spherical chamber

Most of the data in the literature, pertaining to the hydrogen-oxygen reaction, concern experiments performed in spherical silica vessels coated with various salts (11). It was felt desirable to obtain data in a similarly shaped vessel coated with the nickel-nickel phosphide material used throughout the primary chamber, in order to compare the effects of these two types of surfaces on the reaction.

Originally, a spherical chamber one inch in diameter was used but was found to be too small to give reliable data. A three inch diameter chamber was built and observations made of the mixture compositions which resulted in explosion at two temperatures.

The combustion chamber was heated in a conventional electric muffle furnace whose temperature was controlled by a sensitive recording potentiometer (figure 15). The controlling thermocouple, made from chromel and alumel wire, was located in the air space between the furnace windings and the steel cube which formed the chamber. Chamber temperature was measured by means of a portable precision potentiometer connected to another chromel-alumel thermocouple. This thermocouple was embedded to within 1/16 inch of the central three inch spherical cavity in the cube. This measured chamber temperature could be held within $\pm 0.1^{\circ}F$ during a run.

The only successful determinations with this chamber were made along the junction of the first and second explosion limits. As was mentioned previously, the shape of the explosion boundary in this region gives a measure of the surface efficiency in destroying chain carriers, if presented in the proper manner (figure 2). With the chamber at a fixed temperature, these determinations followed this procedure:

1. The chamber and manifold were twice evacuated to a pressure of approximately 0.2 mm Hg and subsequently filled with hydrogen.
2. After a third evacuation, hydrogen was admitted to a low pressure which was measured on an inclined mercury manometer.
3. Oxygen was then admitted and the total pressure at which a "kick" in the manometer occurred was noted.

It was necessary to leave the chamber filled with hydrogen for three to five minutes between runs to obtain reproducible data.

Measurements of the second limit were attempted with this chamber in the conventional manner. Hydrogen is introduced to a pressure above the limit; oxygen is then admitted to get the desired composition, and slow evacuation follows. No successful determinations were made with this technique, however, because of the very large rates of water formation encountered during the unavoidably long manipulation period.

V. EXPERIMENTAL RESULTS

Figures 17 to 21 present the significant results found in this investigation.

Typical reaction chamber pressure vs. time recordings are plotted in figure 17 for several temperatures. The original traces are replotted to simplify the rate determination because the recording system does not use a rectangular coordinate system.

In figure 18 measurements of the rate of water formation are shown vs. temperature, for isothermal heating and a plate spacing of one-half inch. Consistent rates could not be measured above a temperature of about 1510°R due to the large amount of water formed during the manipulation period. Also shown is a curve calculated from a modification of the reaction scheme given in part II.

The rate of pressure decrease observed with gradient heating is shown as a function of the top plate temperature in figure 19. No explosion was observed under these conditions even though the central portion of the hot plate was operated at temperatures as high as 1710°R.

Explosion limit determinations in the spherical chamber are reported in figures 20 and 21. As noted above, it was not possible to obtain explosion data at large partial pressures of oxygen. Shown also in figures 20 and 21 is a comparable curve calculated from the data of other investigators using a vessel coated with sodium hydroxide (5).

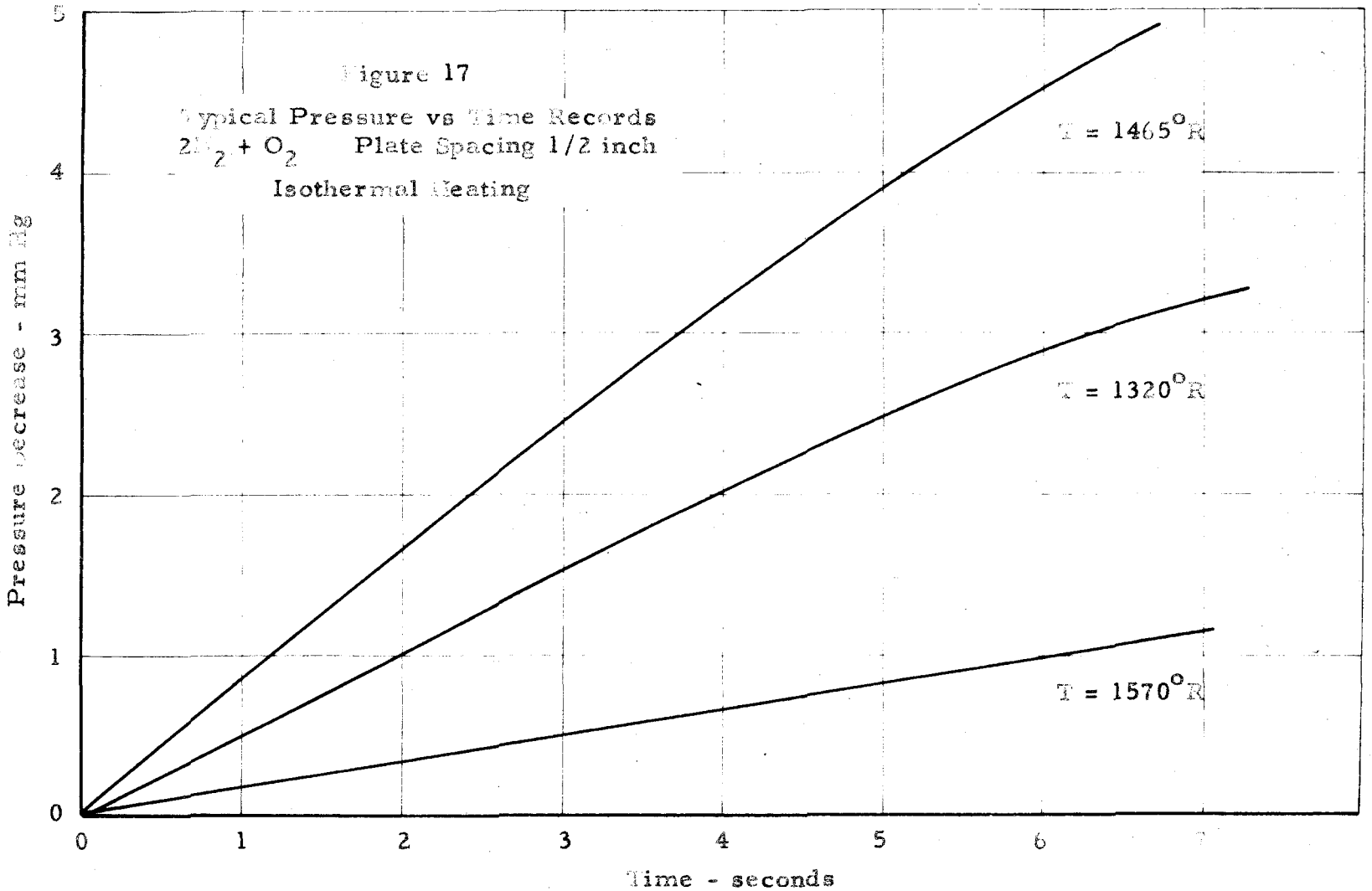
Figure 17
Typical Pressure vs Time Records
$2H_2 + O_2$ Plate Spacing 1/2 inch
Isothermal Heating
T = 1465°R
T = 1320°R
T = 1570°R
Pressure decrease - mm Hg
Time - seconds
0
1
2
3
4
5
6

Figure 18

Reaction Rate vs. Temperature

$2 H_2 + O_2$ Plate Spacing 1/2 inch

Isothermal Heating Pressure 748 mm Hg

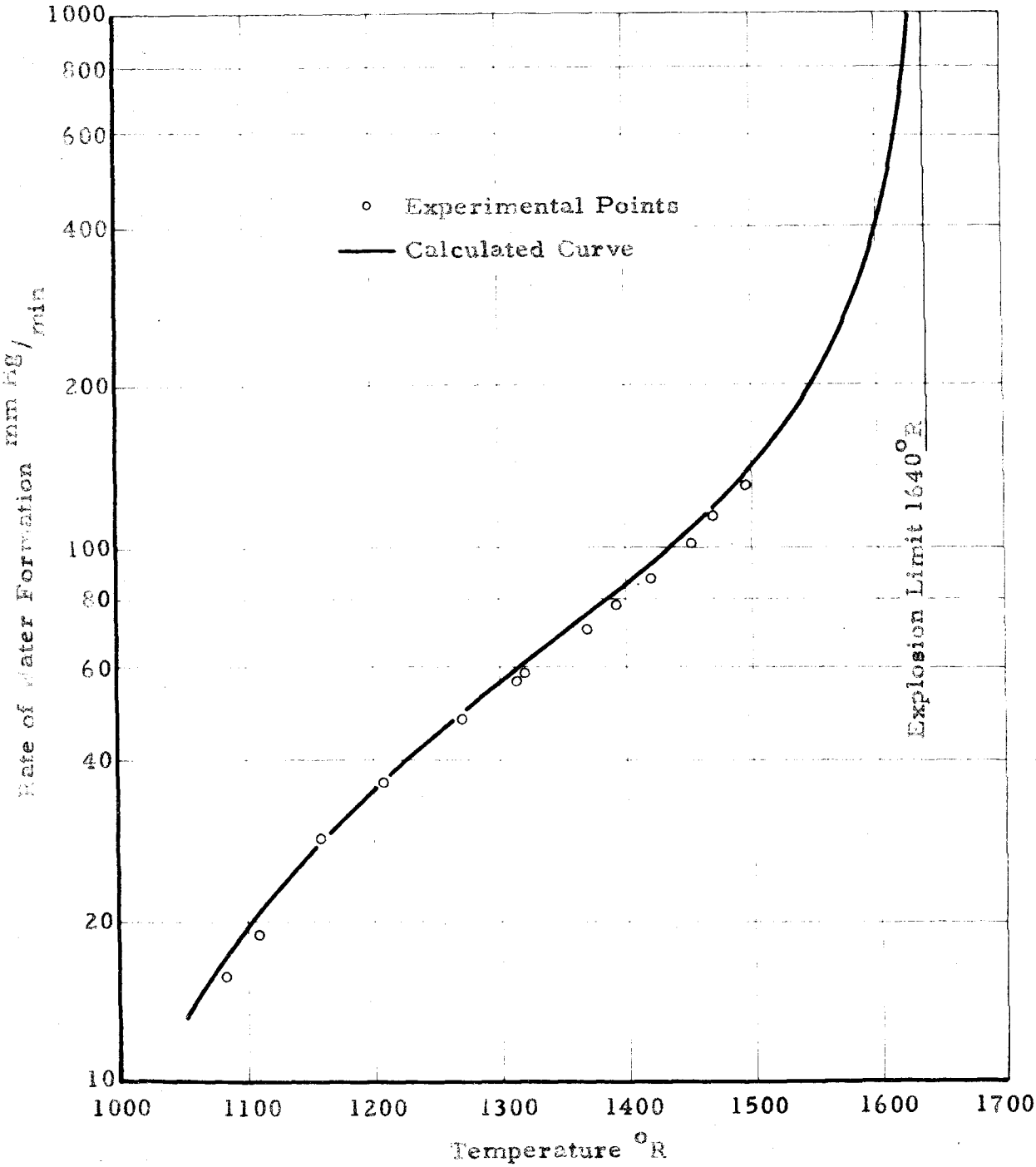

Figure 19

Initial Rate of Pressure Decrease vs. Hot Plate Temperature
Cold Plate Temperature 680°R Plate Spacing 1/2 inch
Stoichiometric Mixture

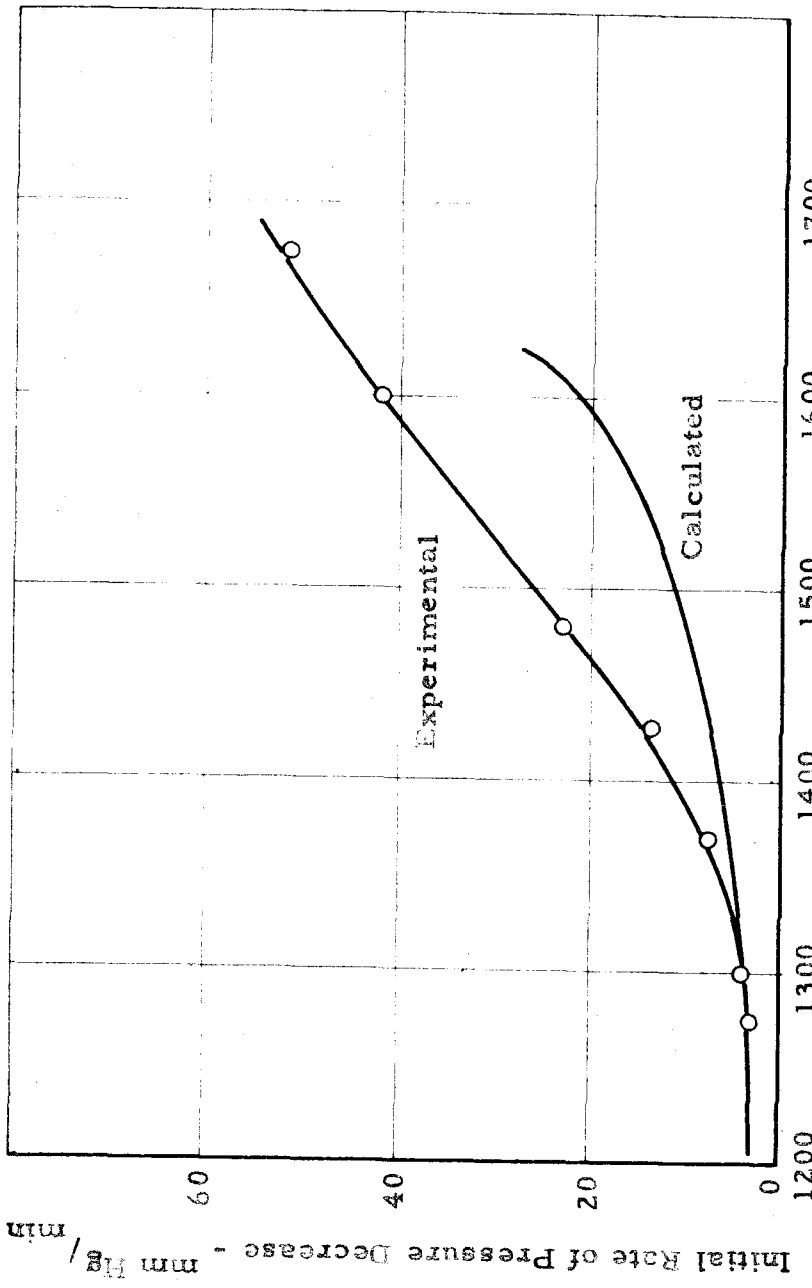

Figure 20

Junction of the First and Second Explosion Limits
Hydrogen-Oxygen Vessel Diameter 3 inches
Temperature = 1490°R

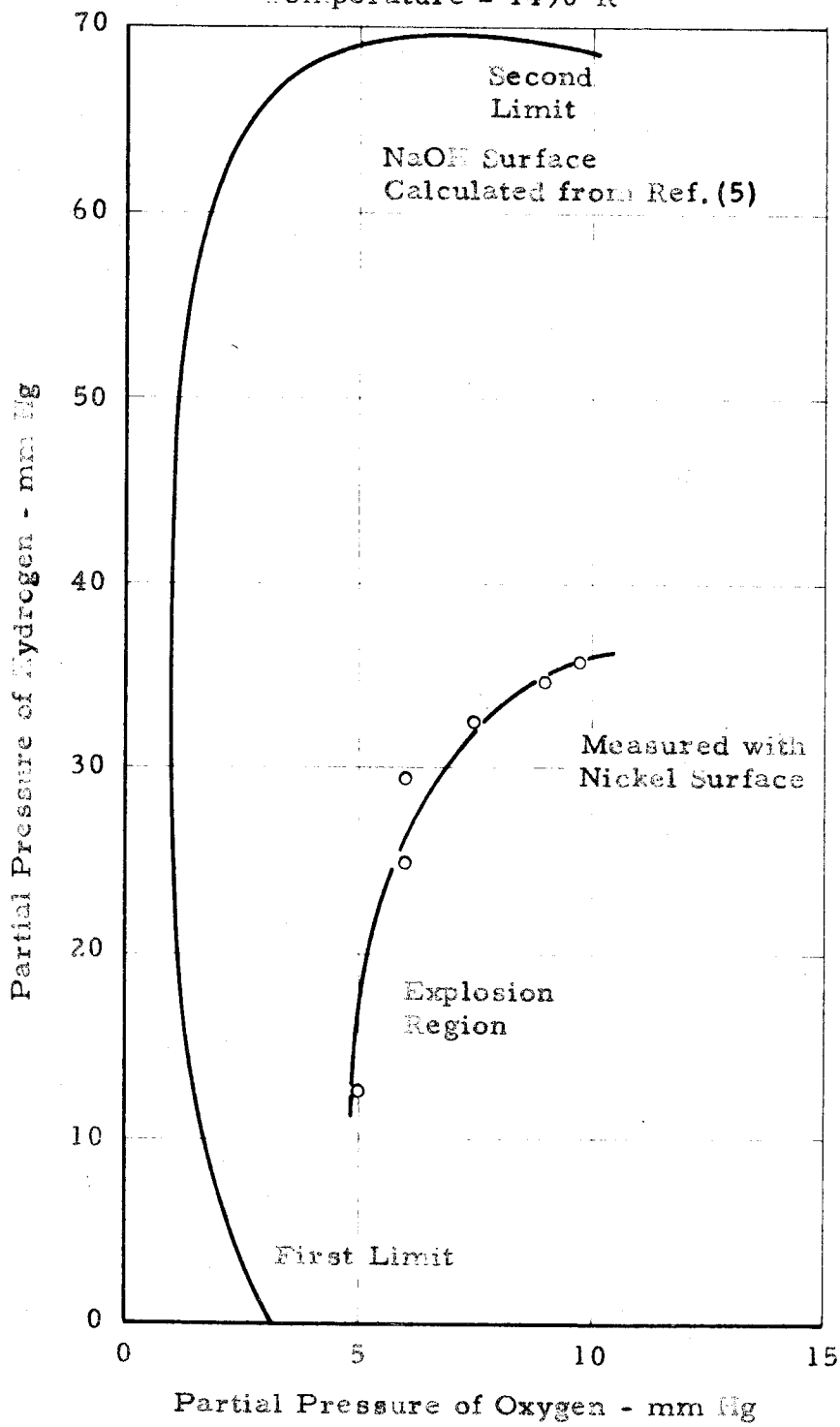

Figure 21

Junction of the First and Second Explosion Limits
Hydrogen-Oxygen Vessel Diameter 3 inches
Temperature = 1440°R

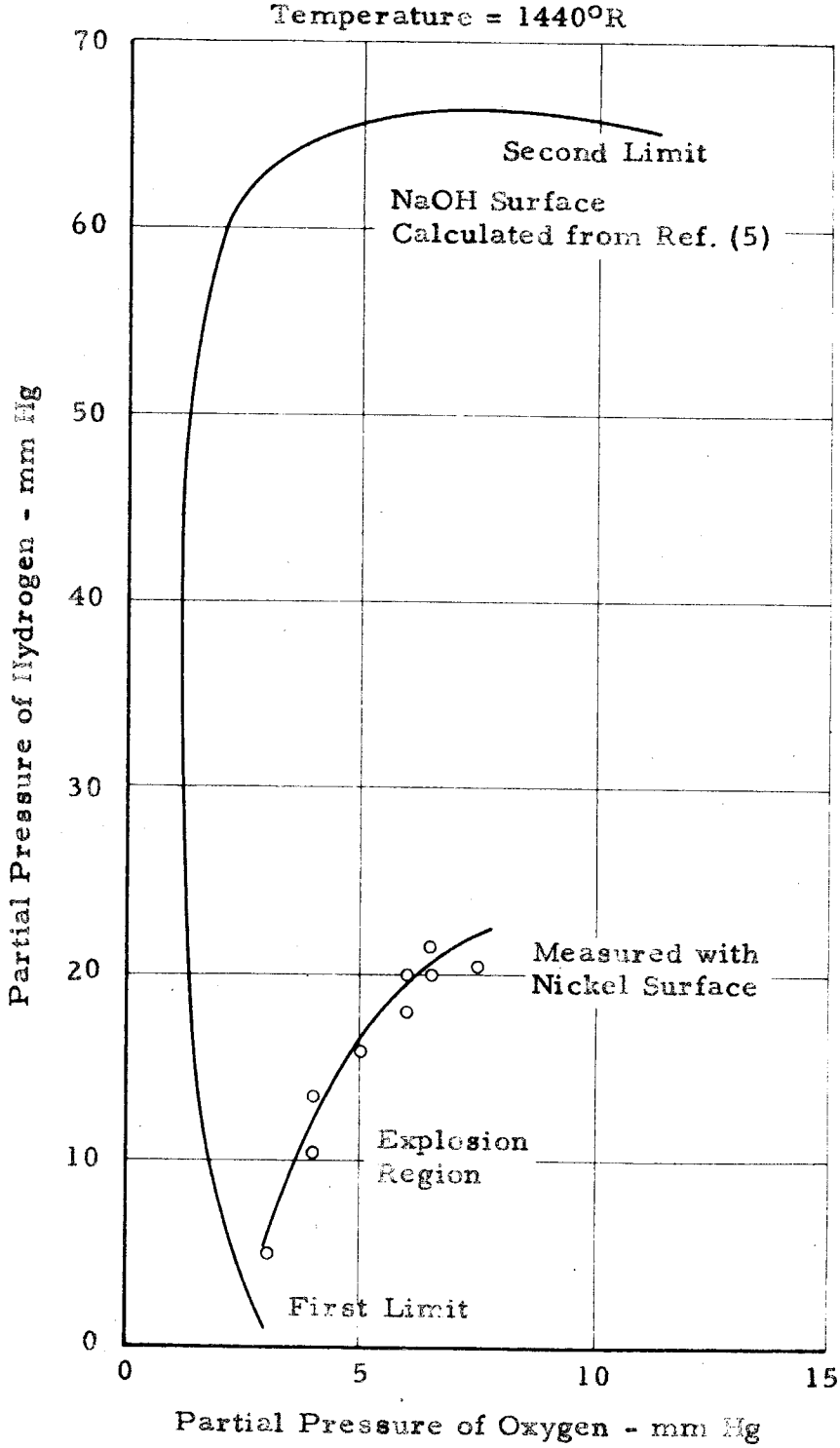

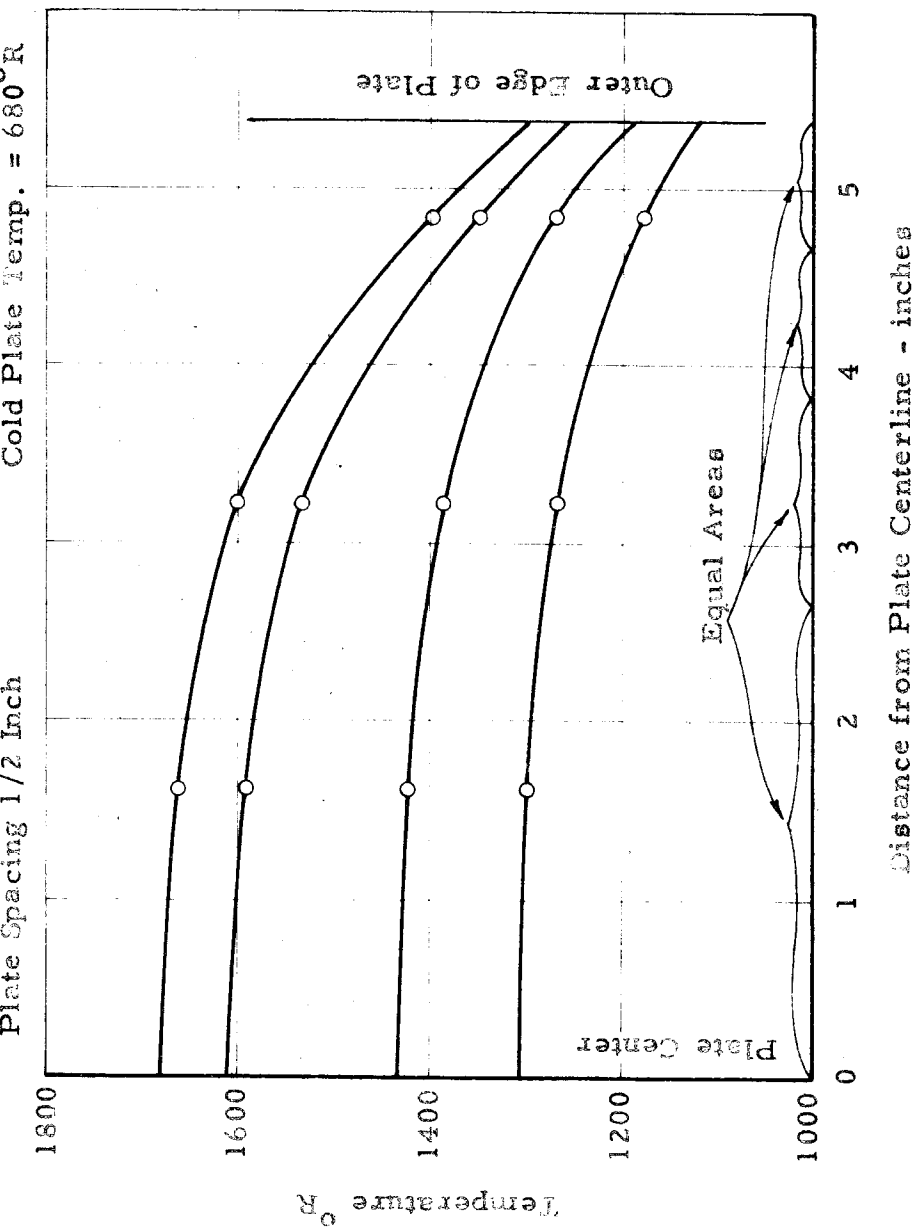

Figure 22

Typical Temperature Profiles Along the Top Plate
With Gradient Heating
Plate Spacing 1/2 Inch Cold Plate Temp. = 680°R

Figure 23

Temperature Distribution Between the Plates
Replotted from reference (3)

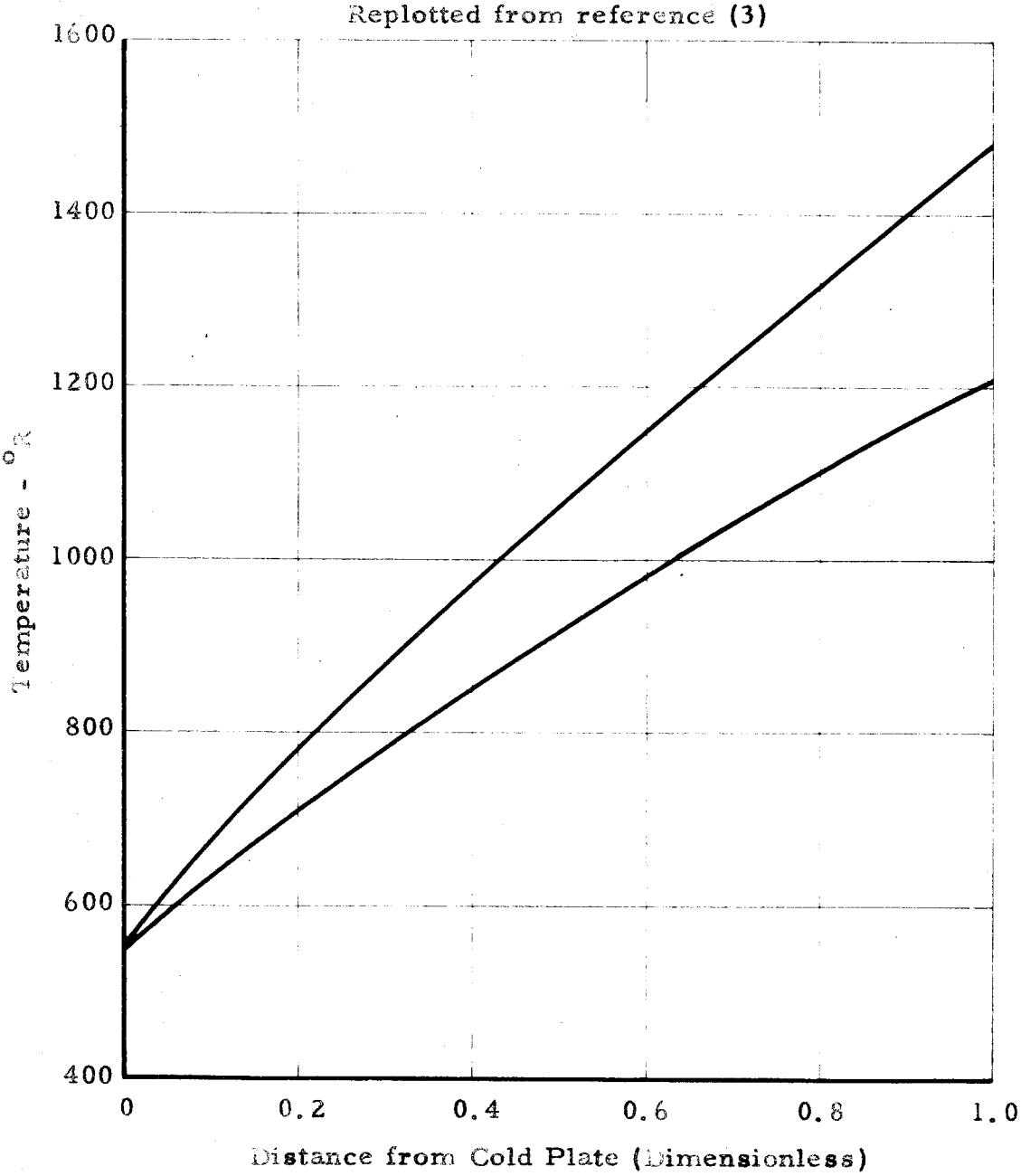

VI. DISCUSSION

Isothermal experiments

The analysis presented in part II indicates that the isothermal explosion limit in the present chamber should be primarily a function of the plate spacing.

Figure 3 presents curves of the explosion temperature of various mixtures of hydrogen, oxygen and water as a function of vessel diameter. These curves were calculated from equations (8) to (16) for a spherical vessel coated with potassium chloride. Also shown are two experimental points indicating the explosion temperature found with plate spacings of 0.5 and 1.5 inches, respectively, in the present chamber. Since these explosions occurred with no time lag after the admission of oxygen, the points have been placed on the curve for no initial water concentration. The explosion points indicated were reproducible within $\pm 2^{\circ}F$. The dependence upon vessel size is exactly as predicted, since the equivalent spherical chamber size changes by the same factor, three, as the plate spacing, between the two points. The "effective diameter" of the chamber appears to be 1.6 times the plate spacing, which is in good agreement with the theoretical value of 2.0 given above. The difference between these two numbers is probably due to the effect of the cylinder walls, since the diameter to plate spacing ratio is really not large enough to consider the plates as being infinite in extent.

The striking feature of the curve in figure 18 is that the experimental rate of water formation remains very large at relatively low temperatures. Indeed, the measured rate at 1100°R corresponds to the rate calculated for the equivalent size spherical chamber, coated with potassium chloride, at 1480°R. Furthermore, the variation of the reaction rate with temperature is much smaller in the nickel chamber. These results are not surprising, since the primary purpose of coating a silica reaction vessel with potassium chloride is to eliminate the occurrence of very large, erratic rates of reaction. Potassium chloride, and even more so, sodium hydroxide, by reducing the rate of water formation during the manipulation period, make the determination of the explosion limits much more reproducible. On the other hand, it has been shown that nickel is an excellent catalyst for the hydrogen-oxygen reaction (12).

For purposes of comparison with the data taken under gradient heating conditions, it is desirable to express the isothermal data, quantitatively, in terms of the fundamental reaction scheme given in equations (8) to (16). Since this mechanism is successful in explaining, quantitatively, the phenomenon observed with hydrogen-oxygen mixtures in salt coated vessels for a wide range of conditions, it might be expected that with a minimum of modification the same scheme would fit the present data.

The explosion temperatures in the present investigation seem to be consistent with the data calculated for a vessel having a

potassium chloride coating, and this fact indicates that the nickel surface is highly effective in destroying chain carriers. Consequently, efforts at modifying the rate equations have been concentrated on the terms which control the low temperature catalytic rate rather than those governing the explosion conditions. It is found that simply by increasing the rate constant of the catalytic surface reaction between hydrogen and oxygen, K_{14}, and modifying its temperature dependence slightly, the previous scheme can be made to give an excellent representation of the present data. The curve in figure 18 is calculated with

$$K_{14} = 46.67 \left(\frac{T}{803}\right)^{3/2} e^{-\left[\frac{2430}{803\,R}\left(\frac{803}{T} - 1\right)\right]} \text{ mm Hg/min} \qquad (40)$$

The only term in equations (10) to (15) that this change affects is s, which becomes

$$s = 49\,d\,\frac{f_{H_2} + 6.88 f_{O_2} + 7.84 f_{N_2}}{f_{H_2} + 0.414 f_{O_2} + 0.454 f_{N_2}}\; e^{+\left[\frac{29070}{803\,R}\left(\frac{803}{T} - 1\right)\right]} \qquad (41)$$

if the same variation with f and d is assumed to be valid as in the case of a salt coated vessel.

Experiments in the spherical chamber shed further light on the characteristics of the nickel surface with regard to chain carrier destruction. In part II it is shown that the shape of the boundary between the explosion and no explosion regions at low pressures, when plotted with the partial pressures of hydrogen and oxygen as coordinates, is a very sensitive indication of the rate of surface chain

destruction. The data presented in reference (5) cover a very wide range of surface materials, and the authors found that sodium hydroxide is among the most effective materials in destroying chain carriers. Furthermore, it was found that some metal surfaces were in this same category but sometimes caused such high rates of reaction during the manipulation period that the explosion limits were unobservable. This latter observation was confirmed in the present investigation by measurements with the nickel spherical chamber, inasmuch as no explosion could be obtained in regions where the required procedure involved holding the mixture at an elevated temperature for more than five seconds. Figures 20 and 21 indicate that the nickel surface is probably much more effective than sodium hydroxide in destroying the chain carriers O and OH, although an accurate comparison between these two systems is difficult, due to the large reaction rate on the nickel surface.

Temperature gradient experiments

The measured rate of pressure decrease as a function of top plate temperature is given for the chamber with gradient heating in figure 19. This curve is in a form for direct comparison with the analysis of the gradient reaction presented in part II. The term $\frac{dn}{dt}$ of equation (39) may be divided into two parts. One part comes from the reaction at the surface, which is at one temperature, while the other part comes from the gas phase reaction occurring over a

range of temperatures. The steps in this calculation are outlined below:

1. The rate constant of the catalytic reaction, equation (40), is subtracted from the measured isothermal rate to give the contribution of the gas phase reaction at any temperature.
2. The change in the number of moles per unit time from the gas phase reaction is calculated in accordance with equation (32) and plotted over the complete range of temperatures existing between the two plates in any particular gradient test.
3. A linear temperature variation between the plates is assumed, since previous measurements (3) indicate that this is a good approximation (figure 23). The curve obtained in step two is then integrated graphically across the chamber to obtain the portion of $\frac{dn}{dt}$ due to the gas phase reaction.
4. The change in the number of moles per unit time and per unit surface area is computed as a function of temperature from equation (40) and the total surface area of the chamber. Since it is not possible to maintain the hot plate at a

uniform temperature (figure 22) the rate of the surface reaction is calculated as an average of the rates at the mean temperature of four equal area annuli forming the surface of the plate. This calculation yields the second portion of the term $\frac{dn}{dt}$.

The overall rate of pressure decrease, calculated as indicated, is shown in figure 19 for comparison with the measured rate. It is seen that at low surface temperatures, where the reaction is almost completely catalytic, the two curves merge. The fact that they diverge markedly as the surface temperature is raised is not surprising, since it is almost certain that the active chain carriers, formed at high temperatures, diffuse into the relatively cold gas and thereby raise the rate of reaction in these regions. In other words, the second assumption concerning this calculation, listed in part II, is evidently not valid at temperatures above $1300^{\circ}R$.

No spontaneous explosion was ever observed in either the present gradient tests or those made previously by Schurman. It is felt that the explanation of this fact, as well as Schurman's other observations, which were summarized earlier, lies in the exceptional inhibiting effect which water has on the hydrogen-oxygen reaction. There is no doubt that some water is formed during the flow process occurring in these earlier tests. At $1615^{\circ}R$ Schurman estimated from his interference patterns that the mixture might consist of as

much as 50% water vapor. Under these conditions, from figure 3 it can be seen that the mixture should not be expected to explode with a surface temperature of only 1710°R. The concentration gradient which was observed in this previous work was undoubtedly due to a high initial rate of reaction near the hot plate after the flow was shut off. That the reactants were not consumed after three minutes is due to the drastic reduction in rate which this initial formation of water causes. When the mixture is pulsed with gas, under these conditions, the effective water concentration is reduced and an explosion results.

In the present investigation, sampling tests indicate that the reaction proceeds to within 5% of completion in approximately two minutes, with the hot plate above 1500°R. The catalytic effect of the nickel surfaces in this work probably accounts for the difference between this fact and the previous observation that the mixture could be made to explode after three minutes residence time. No evidence of hydrogen peroxide was ever found by analysis of the products from this completed reaction, even though the technique for this determination was capable of detecting less than 3% of this constituent. However, it is difficult, on the basis of these tests, to conclude anything regarding the role which hydrogen peroxide might play in the intermediate reaction steps, since its rate of decomposition is probably high under the conditions within the chamber.

VI. CONCLUSIONS

The rate of reaction between hydrogen and oxygen in a combustion chamber with nickel surfaces and unusual geometry can be described quantitatively in terms of the well established mechanism of this reaction found in other types of systems. The dependence of both the reaction rate and the explosion temperature upon vessel size has been confirmed. A relatively large catalytic reaction occurs at the nickel surface and persists at temperatures below 1100°R. The chain destructiveness of the surface used appears to be high for the chain carriers normally associated with this reaction.

When a hydrogen-oxygen mixture reacts in a strong temperature gradient at temperatures below 1300°R the observed rate of pressure decrease can be explained quantitatively by a simplified theory utilizing data obtained under isothermal conditions. At higher temperatures, the observed pressure decrease can be accounted for, qualitatively, by the diffusion of chain carriers formed in the hot gas into colder regions. The absence of an explosion with hot plate temperatures as high as 1710°R is caused by the strong inhibiting effect which water vapor has on the chain reaction.

APPENDIX

Commercial equipment list

A. Pressure recording

1. Statham pressure transducers, model numbers:
   P25-25D-240
   P58-0.2D-335
   P112-0.7D-430
2. Brush Universal Analyzer Model BL-320
3. Brush Recording Oscillograph Model BL-222
4. Indicating meter: Simpson Model 260
5. Wallace and Tiernan precision mercury manometer.

B. Temperature controlling

1. Chromalox 1/2 inch tubular, alloy sheath heaters
2. Leeds and Northrup Speedomax Type G
   eight-point recording potentiometer.
   Range 0-1500°F.
3. Powerstat Type 1226 0-270 volt autotransformers.
4. Braun Corp. muffle furnace type Mu-55
5. Leeds and Northrup Micromax extended range
   recording controller. Least division 0.01 mv.
6. Leeds and Northrup Portable precision potentiometer,
   type 8662.

REFERENCES

(1) B. Lewis and G. von Elbe, J. Chem. Phys., (1942), Vol. 10, p. 366.

(2) Sir Alfred Egerton and D. R. Warren, Proc. Roy. Soc. A, (1951), Vol. 204, p. 465.

(3) G. A. Schurman, Ph.D. thesis, (1950), California Institute of Technology,

(4) K. J. Laidler, "Chemical Kinetics", (1950), Mc Graw-Hill Book Co., New York, p. 180.

(5) D. R. Warren, Proc. Roy. Soc. A, (1952), Vol. 211, p. 86.

(6) B. Lewis and G. von Elbe, "Combustion, Flames and Explosions", (1951), Academic Press, New York, p. 20.

(7) N. Semenov, Acta Physicochim (U.R.S.S.), (1943), Vol. 18, p. 93.

(8) M. J. Henkel, H. Hummel, and W. P. Spaulding, Third Symposium on Combustion, Flame and Explosion Phenomena, (1949), Williams and Wilkins Co., Baltimore, p. 135.

(9) F. A. Schwertz, and J. E. Brow, J. Chem. Phys., (1951), Vol. 19, p. 640.

(10) B. Lewis and G. von Elbe, Third Symposium on Combustion, Flame and Explosion Phenomena, (1949), Williams and Wilkins Co., Baltimore, p. 488.

(11) R. N. Pease, J. Am. Chem. Soc., (1930), Vol. 52, p. 5106.

(12) P. H. Emmett, "Catalysis", (1954), Vol. 1, Reinhold Publishing Co., New York, p. 160.